

368

VES

7000019



NATIONAL AERONAUTICS AND SPACE ADMINISTRATION

MSC INTERNAL NOTE NO. EB-R-68-11

18 OCTOBER 1968



AN FM OPTIMIZATION STUDY FOR THE APOLLO UNIFIED S-BAND TELECOMMUNICATIONS SYSTEM

By F. J. Loch

INFORMATION SYSTEMS DIVISION MANNED SPACECRAFT CENTER HOUSTON, TEXAS

N70-35793

(ACCESSION NUMBER)

(THRU)

(PAGES)

(CODE)

(NASA CR OR TMX OR AD NUMBER)

(CATEGORY)

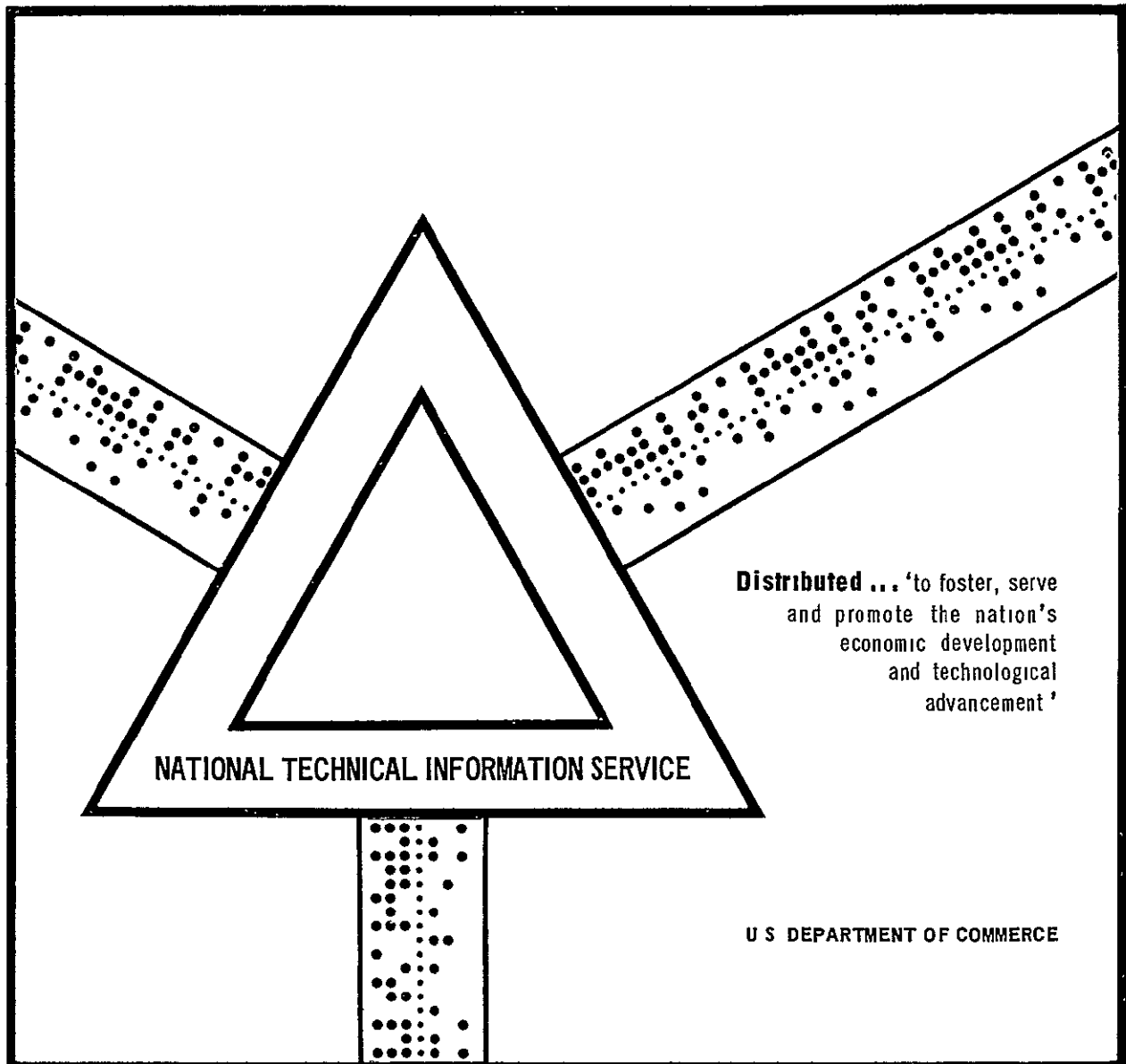
FACILITY FORM 602

Reproduced by NATIONAL TECHNICAL INFORMATION SERVICE Springfield, Va. 22151

N70-35793

AN FM OPTIMIZATION STUDY FOR THE APOLLO UNIFIED S-BAND TELECOMMUNICATIONS SYSTEM

Manned Spacecraft Center
Houston, Texas



MSC INTERNAL NOTE NO. EB-R-68-11

AN FM OPTIMIZATION STUDY FOR THE
APOLLO UNIFIED S-BAND TELECOMMUNICATIONS SYSTEM

Prepared by Frank J. Loch
F J Loch
Applied Analysis Section

Approved by G. D. Arndt
G. D Arndt
Head, Applied Analysis Section

R W Moorehead
R W Moorehead
Chief, Systems Analysis Branch

Approved for
Distribution P H Vavra
P H Vavra
Chief, Information Systems Division

NATIONAL AERONAUTICS AND SPACE ADMINISTRATION
MANNED SPACECRAFT CENTER
INFORMATION SYSTEMS DIVISION
SYSTEMS ANALYSIS BRANCH
18 OCTOBER 1968

ACKNOWLEDGEMENTS

The author wishes to thank Mr William M Conrad of the Philco-Ford Corporation, Education and Technical Services Division, for his valuable contributions to the FM optimization study. Mr Conrad is credited with the circuit design of the click detection and eliminator threshold extension device discussed in this document. Mr Conrad also made valuable contributions to the test program that resulted in the data and photographs presented in this document.

TABLE OF CONTENTS

<u>Section</u>	<u>Page</u>
1	INTRODUCTION
1 1	Purpose 1-1
1.2	Theoretical And Experimental Approach . . . 1-1
2	SUMMARY 2-1
3	FM THRESHOLD
3 1	General 3-1
3 2	Click Event 3-5
3.3	FM Demodulator Performance With Click Noise 3-15
3 4	Click Symmetry 3-27
4	THRESHOLD EXTENSION TECHNIQUES
4.1	General 4-1
4 2	Click Detection 4-1
4 3	Click Elimination 4-7
4 4	Threshold Extension Device 4-10
5	EXPERIMENTAL RESULTS
5 1	General 5-1
5 2	Signal-Plus-Noise Waveform Analysis 5-2
5 3	Signal-to-Noise Ratio Tests 5-11
5 3 1	CSM FM Modes 1 and 2 5-11
5 3 2	CSM FM Mode 4 5-15
5 4	Word Intelligibility Tests 5-21
5 5	Television Picture Quality Analysis 5-26
 <u>Appendix</u>	
A	BIBLIOGRAPHY A-1
B	ABBREVIATIONS AND SYMBOLS B-1

LIST OF FIGURES

<u>Figure</u>		<u>Page</u>
3-1	Graphical Determination of FM Threshold For A Typical Demodulator SNR Transfer Curve . . .	3-2
3-2	FM demodulator Output Noise Characteristics . . .	3-3
3-3	Phasor Representation of A, X, Y, R and N	3-6
3-4	Phasor Representation of Noise, Carrier, and Resultant R, Near FM Threshold	3-7
3-5	Relationship Between $\pm 2\pi$ Phase Excursions and Resulting Impulses of Area 2π	3-9
3-6	First Order Click Waveform	3-10
3-7	First Order Click Waveform	3-10
3-8	Second Order Click Waveform	3-11
3-9	Second Order Click Waveform	3-11
3-10	Third Order Click Waveform	3-12
3-11	Third Order Click Waveform	3-12
3-12	Fourth Order Click Waveform	3-13
3-13	Fourth Order Click Waveform	3-13
3-14	Effect of Carrier Offset on Click Noise Distribution	3-28
3-15	Output Noise Power Increase vs Center Frequency Offset	3-29
4-1	Demodulated Signal Plus Noise Waveform With and Without Postdetection Filtering ($f_m = 10$ KHz). . .	4-2
4-2	Demodulated Signal Plus Noise Waveform With and Without Postdetection Filtering ($f_m = 10$ KHz). . .	4-2
4-3	Demodulated Signal Plus Noise Waveform With and Without Postdetection Filtering ($f_m = 50$ KHz). . .	4-3
4-4	Demodulated Signal Plus Noise Waveform With and Without Postdetection Filtering ($f_m = 50$ KHz). . .	4-3

LIST OF FIGURES (CONT'D)

<u>Figure</u>		<u>Page</u>
4-5	Demodulated Signal Plus Noise Waveform With and Without Postdetection Filtering ($f_m = 100$ KHz) .	4-4
4-6	Demodulated Signal Plus Noise Waveform With and Without Postdetection Filtering ($f_m = 100$ KHz) .	4-4
4-7	Click Detector Block Diagram	4-6
4-8	Click Eliminator Block Diagram	4-8
4-9	Click Detection and Elimination Threshold Extension Device Configuration	4-9
5-1	Signal Plus Noise Waveform Analysis Test Configuration	5-3
5-2	Signal Plus Noise Waveform Analysis	5-4
5-3	Signal Plus Noise Waveform Analysis	5-4
5-4	Signal Plus Noise Waveform Analysis	5-5
5-5	Signal Plus Noise Waveform Analysis	5-5
5-6	Signal Plus Noise Waveform Analysis	5-6
5-7	Signal Plus Noise Waveform Analysis	5-6
5-8	Signal Plus Noise Waveform Analysis	5-7
5-9	Signal Plus Noise Waveform Analysis	5-7
5-10	Signal Plus Noise Waveform Analysis	5-8
5-11	Signal Plus Noise Waveform Analysis	5-8
5-12	Signal Plus Noise Waveform Analysis	5-9
5-13	Signal Plus Noise Waveform Analysis	5-9
5-14	Test Configuration For CSM Modes 1 and 2 Signal-to-Noise Ratio Tests With and Without Threshold Extension Device	5-12
5-15	Output SNR vs Input SNR For 1 1 CSM Playback Voice Mode	5-13

LIST OF FIGURES (CONT'D)

<u>Figure</u>		<u>Page</u>
5-16	Output SNR vs Input SNR For 32.1 CSM Playback Voice Mode	5-14
5-17	Output SNR Improvement vs Input SNR For 1 1 and 32 1 CSM Playback Voice	5-16
5-18	Configuration For CSM Mode 4 SNR Tests	5-17
5-19	Output SNR vs Input SNR For CSM FM Mode 4	5-18
5-20	Output SNR Improvement vs Input SNR For CSM FM Mode 4 With Click Elimination	5-20
5-21	Configuration For CSM FM Mode 1 Word Intelligibility Tests With and Without Threshold Extension Device	5-22
5-22	Percent Word Intelligibility vs Input SNR For 1 1 CSM Playback Voice Mode	5-23
5-23	Configuration For CSM FM Mode 2 Word Intelligibility With and Without Threshold Extension Device	5-24
5-24	Percent Word Intelligibility vs Input SNR For CSM 32 1 Playback Voice Mode	5-25
5-25	Configuration For CSM Mode 4 Television Picture Quality Tests	5-27
5-26	CSM Mode 4 TV Picture Quality Tests	5-28
5-27	CSM Mode 4 TV Picture Quality Tests	5-28
5-28	CSM Mode 4 TV Picture Quality Tests	5-29
5-29	CSM Mode 4 TV Picture Quality Tests	5-29
5-30	CSM Mode 4 TV Picture Quality Tests	5-30
5-31	CSM Mode 4 TV Picture Quality Tests	5-30
5-32	CSM Mode 4 TV Picture Quality Tests	5-31
5-33	CSM Mode 4 TV Picture Quality Tests	5-31

LIST OF FIGURES (CONT'D)

<u>Figure</u>			<u>Page</u>
5-34	CSM Mode 4	TV Picture Quality Tests	5-33
5-35	CSM Mode 4	TV Picture Quality Tests	5-33
5-36	CSM Mode 4	TV Picture Quality Tests	5-34
5-37	CSM Mode 4	TV Picture Quality Tests	5-34
5-38	CSM Mode 4	TV Picture Quality Tests	5-35
5-39	CSM Mode 4	TV Picture Quality Tests	5-35
5-40	CSM Mode 4	TV Picture Quality Tests	5-36
5-41	CSM Mode 4	TV Picture Quality Tests	5-36

LIST OF TABLES

<u>Table</u>		<u>Page</u>
1-1	Marginal Apollo Down-Link FM Modes	1-2
2-1	Threshold Extension Device Performance Summary . . .	2-3
3-1	Duration and Amplitude Characteristics of Nth Order Click Waveforms	3-14
5-1	CSM Modes Used For Threshold Extension Device Test	5-1

SECTION 1

INTRODUCTION

1 1 PURPOSE

An analysis of the Apollo Unified S-Band (USB) communications system¹, performed by the Information Systems Division, Manned Spacecraft Center, has indicated that certain down-link FM modes exhibit negative circuit margins at lunar distance for worst case conditions. A negative margin implies that the operational requirements will not be met for the affected modes. The three FM modes that were found to have negative margins are listed in Table 1-1 with their respective channel characteristics.

As a result of these findings, an intensive study of optimization techniques was conducted by ISD/MSD for the purpose of improving the performance of the marginal FM modes. This optimization study resulted in the development of an FM threshold extension device that could be used to provide improved performance for the Apollo Manned Spaceflight Network (MSFN) carrier frequency demodulator. By extending the threshold operation of the MSFN demodulator, it is possible to obtain better circuit margins for the affected FM modes.

The purpose of this document is to present the results of the FM optimization study which resulted in the development of the threshold extension device. This document also presents and evaluates test data representing the performance of the device when it is used in conjunction with an MSFN receiver.

1 2 THEORETICAL AND EXPERIMENTAL APPROACH

An analysis of the FM threshold phenomena based on the earlier work of S. O. Rice² is presented. The results of this analysis show that the presence of impulse noise in the output of a demodulator is a primary factor causing threshold in an FM system.

¹C. Dawson, *A Performance Analysis of the Apollo Unified S-Band Communications System for a Typical Lunar Mission* (MSC Internal Note MSC-EB-R-67-1, August 1967)

²S. O. Rice, "Noise in FM Receivers," *Proceedings, Symposium on Time Series Analyses*, ed. M. Rosenblatt (New York, 1963)

TABLE 1-1

MARGINAL APOLLO DOWN-LINK FM MODES

MODE	SERVICE(S)	SPECIFIED CARRIER FREQUENCY DEVIATION (Δf) (KHZ)			WORST CASE MODE-AS-A-WHOLE CIRCUIT MARGIN (DB) 215,000 NM	MODULATION FREQUENCY
		WORST	NOMINAL	BEST		
CSM MODE 1	1 1 PLAYBACK OF VOICE	60	100	120	-0 7	300-3000 HZ
	1 1 PLAYBACK CSM 51 2 KBPS TLM	510	600	690		1 024 MHZ (SUBCARRIER)
CSM MODE 2	32 1 PLAYBACK OF VOICE	60	100	120	-0 7	9600-96,000 HZ
	32 1 PLAYBACK CSM 1 6 KBPS TLM	510	600	690		1 024 MHZ (SUBCARRIER)
CSM MODE 4	TV	0 9	1 0	1 1	-0 7	0-500 KHZ

1 2 THEORETICAL AND EXPERIMENTAL APPROACH (Cont'd)

The threshold extension technique is based on the elimination of noise impulses in the demodulator output. An amplitude detection technique is used to obtain information for the noise elimination circuits that operate on a delayed output of the demodulator.

SECTION 2

SUMMARY

The performance of an FM demodulator can be defined in terms of the threshold phenomena, which determines the minimum acceptable input signal-to-noise ratio for the system. The presence of high amplitude noise impulses (click noise) in the demodulator output is a primary factor contributing to the occurrence of threshold in an FM system. Certain distinguishing characteristics of click noise provide a basis for practical techniques that can be implemented at the output of an FM demodulator to improve its threshold performance.

A threshold extension device has been developed that operates on the principle of click detection and elimination. The device was designed to be compatible with the MSFN ground station receiver and to improve the performance of the Apollo Unified S-Band Communications System.

Previous work in the area of FM demodulator improvement has been concentrated on the design of specialized demodulation schemes that provide optimum performance for one set of channel parameters. The Apollo down-link FM modes, however, use several channels having different characteristics in terms of required channel bandwidth, maximum frequency deviation, and range of modulation frequencies.

The click noise eliminator offers an advantage in flexibility since it is not a demodulator but, rather, a device which can be implemented at the output of any FM discriminator to provide improved system performance. The presence of unsymmetrical click noise in the demodulator output, resulting from offsets in carrier frequency, does not affect the performance of the device.

Photographs of demodulated Apollo television pictures comparing the unprocessed demodulator output with the click-eliminated output are presented to illustrate the effectiveness of the threshold extension technique.

.2 SUMMARY (Cont'd)

Additional data obtained from tests of the Apollo playback voice modes reflect the output signal-to-noise ratio improvement in the form of increased voice intelligibility scores. Improvements of 15 percent to 20 percent in word intelligibility scores are obtained when the device is used at the output of the Apollo MSFN receiver.

Experimental results using the Apollo television and playback voice modes have shown that the click elimination device provides an improvement in output signal-to-noise ratio of 6 dB to 10 dB. This improvement in output signal-to-noise ratio corresponds to a 1.5 dB to a 2.0 dB extension of threshold.

The performance characteristics of the threshold extension device are summarized in Table 2-1.

The values listed in Table 2-1 are based on the improvement obtained when the device was used at the output of an Apollo MSFN phase lock loop (PLL) demodulator. The threshold extension obtained was in addition to the normally expected improvement of a PLL demodulator over a standard FM discriminator. The device was also tested with a frequency modulation feedback (FMFB) discriminator, and similar values of threshold extension were obtained. Therefore, the threshold extension technique is capable of improving the performance of any FM demodulation scheme that is degraded by the presence of click noise in the output.

A breadboard version of the threshold extension device was used for the tests referenced in this document. Work is presently underway to complete a refined click detection and elimination device that uses integrated circuits to improve performance. It is expected that the finalized version of the threshold extension device will provide additional SNR improvement.

The following steps must be followed to insure optimum performance of the click elimination device:

- A. The threshold level of the click detector must be set as close as possible to the modulation peaks to insure maximum click detection efficiency.
- B. The click-eliminator cutoff time must equal the click duration. The click duration is determined by the bandwidth of the preclick-detection filter. An optimum low pass bandwidth of 2 MHz was used for the Apollo modes.

TABLE 2-1

THRESHOLD EXTENSION DEVICE PERFORMANCE SUMMARY

CSM MODE	SERVICE	MAXIMUM OUTPUT SNR IMPROVEMENT (DB)	THRESHOLD EXTENSION (DB)	INPUT SNR FOR MAXIMUM IMPROVEMENT	EFFECTIVE INPUT SNR OPERATING RANGE	COMMENTS
1	1 1 PLAYBACK VOICE	10 DB	2 0 DB	3.3 DB	0 TO 10 DB	MAXIMUM WORD INTELLIGIBILITY IMPROVEMENT OF 25% WAS OBTAINED
2	32 1 PLAYBACK VOICE	7 5 DB	1 5 DB	4.0 DB	0 TO 10 DB	MAXIMUM WORD INTELLIGIBILITY IMPROVEMENT OF 4% WAS LIMITED BY INHERENT RECORDING-PLAYBACK DISTORTION.
4	TELEVISION	7 5 DB	1 5 DB TO 2 0 DB	3 0 DB	0 TO 10 DB	THRESHOLD EXTENSION IS OBSERVED BY COMPARING OUTPUT VIDEO PICTURES WITH AND WITHOUT CLICK ELIMINATION

2 SUMMARY (Cont'd)

- C The beginning of the click-eliminator cutoff must coincide exactly with the beginning of the click in the demodulator output
- D The recovery time for the click detection and elimination circuits must be made as small as possible to insure efficient operation at high click rates

SECTION 3

FM THRESHOLD

3 1 GENERAL

By definition, the criteria for evaluating the performance of an FM demodulator is based on *the ability of the device to provide a linear relationship between the output and input signal-to-noise ratios*. The useful operating range of all FM demodulators, however, is limited by the fact that this relationship, or transfer characteristic, becomes non-linear below a certain value of input signal-to-noise ratios. This value of input SNR is called the "point of threshold" for the demodulator.

Since it is difficult in most cases to determine the exact value of input SNR that divides the linear and non-linear regions of the performance curve, it is necessary to define a reasonable criteria for determining the threshold point.

One accepted definition of FM threshold is based on the graphical determination of the specific input SNR value whose corresponding output SNR occurs exactly 1 dB below an extension of the linear portion of the transfer curve. This method of defining FM threshold is illustrated in Figure 3-1 and will be used consistently throughout this document.

The occurrence of threshold in an FM system can also be defined in terms of the demodulator output noise characteristics. In general, when the demodulator is operating with values of input SNR greater than 10 dB, the output noise spectrum is parabolic, and the amplitude distribution is Gaussian. As the input SNR decreases, the output noise voltage is punctuated with occasional high amplitude noise spikes having either positive or negative polarity. These noise impulses become more frequent as the input SNR is reduced to values below 10 dB. For the region of input SNR's between 0 dB and 10 dB, the output noise power increases at such a rate that the slope of the SNR transfer curve becomes much more severe than the slope of the linear portion. This implies that a small change in input SNR results in a relatively large change in output SNR as illustrated in Figure 3-1. The difference in the relative contribution of Gaussian noise and click noise can be seen by noting their individual spectral characteristics in Figure 3-2.

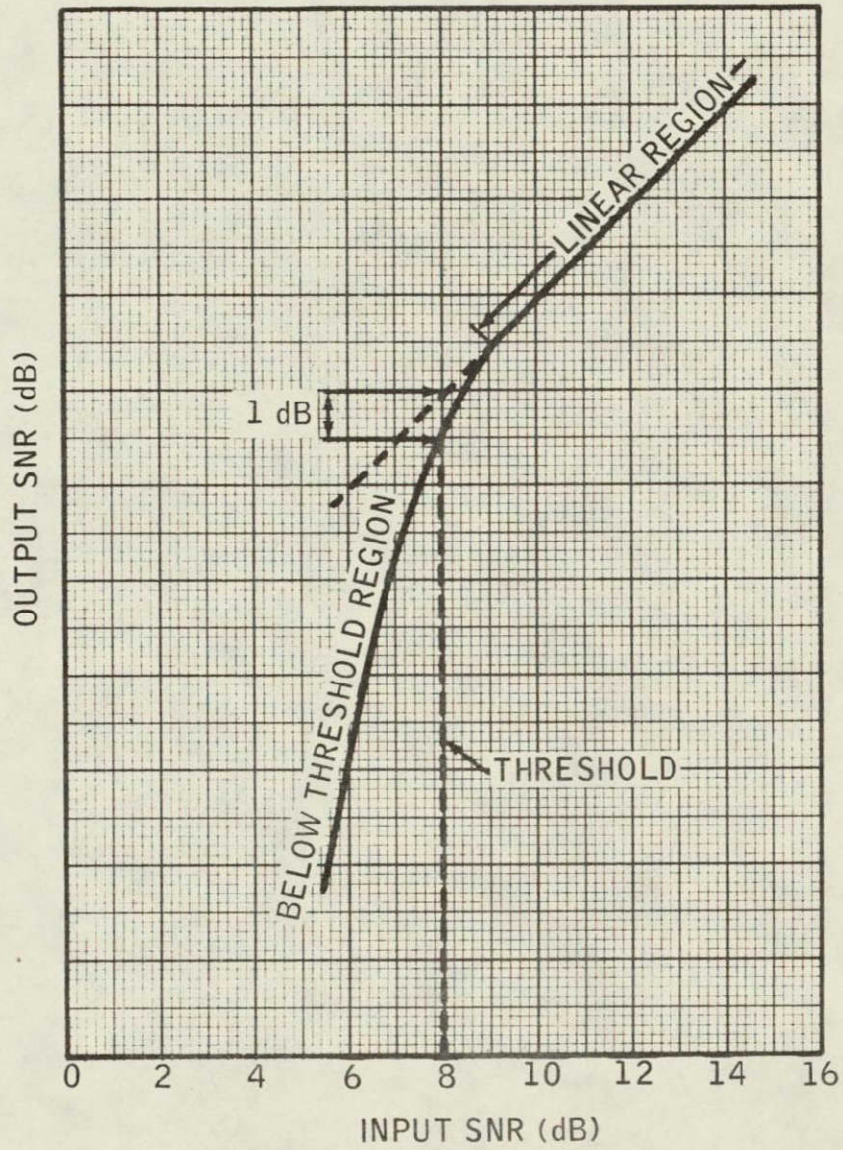
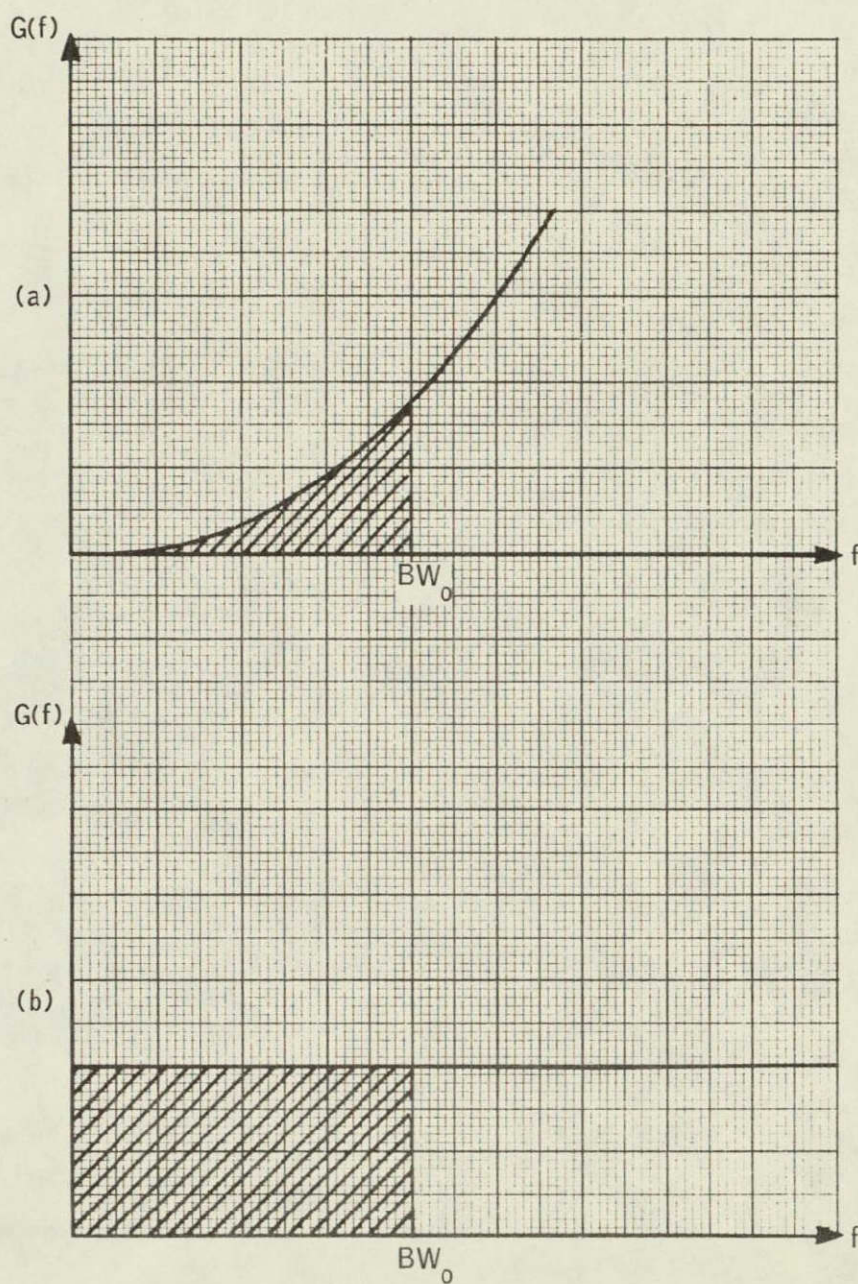


Figure 3-1 Graphical Determination of FM Threshold for a Typical Demodulator SNR Transfer Drive



(a) BASEBAND NOISE SPECTRUM ABOVE THRESHOLD
 (b) CLICK NOISE SPECTRUM BELOW THRESHOLD

GC10177(A)-39

Figure 3-2 FM Demodulator Output
 Noise Characteristics

3.1 GENERAL (Cont'd)

The energy contained in the individual noise spikes (called click noise) at the output of an FM demodulator contributes significantly to the total output noise power. In addition, the impulsive nature of click noise causes it to be much more degrading to the demodulated signal than the Gaussian output noise. Although click noise is not the only phenomena which causes FM threshold, it is definitely a primary factor contributing to the occurrence of threshold in an FM system.

3.2 CLICK EVENT

Consider an unmodulated signal at the input of an ideal FM discriminator where the carrier is represented as $G(t)$.

$$G(t) = A \cos \omega_c t \quad (1)$$

The input noise to the discriminator can be represented in quadrature form by the following expression:

$$N(t) = X(t) \cos \omega_c t + Y(t) \sin \omega_c t \quad (2)$$

where $X(t)$ and $Y(t)$ are independent random variables. Therefore, the total input carrier plus noise is

$$G(t) + N(t) = [A + X(t)] \cos \omega_c t + Y(t) \sin \omega_c t \quad (3)$$

which can also be expressed as follows

$$G(t) + N(t) = R \cos [\omega_c t + \phi(t)] \quad (4)$$

where R is defined as the magnitude of the resultant carrier plus noise waveform, ω_c is the carrier frequency, and ϕ is the phase of the resultant R with respect to the carrier. The FM demodulator detects the frequency of the signal by differentiating the phase of the received signal plus noise. The phase of the signal-plus-noise waveform can be obtained from equation (3).

$$\phi = \tan^{-1} \frac{Y}{A+X} \quad (5)$$

3.2 CLICK EVENT (Cont'd)

For high signal-to-noise ratios, we can assume that $A \gg X$. Therefore,

$$\phi = \tan^{-1} \frac{Y}{A} \doteq \frac{Y}{A} \quad (6)$$

The following phasor relationship exists between A , X , Y , R , N and ϕ , as shown in Figure 3-3.

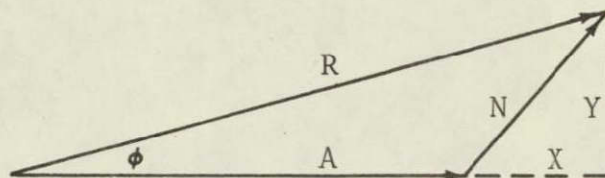


Figure 3-3 Phasor Representation of A , X , Y , R , and N

X and Y are Gaussian distributed random variables whose fluctuation causes the angle ϕ to change accordingly.

The click event takes place at the input of the FM discriminator as an interaction between the randomly varying noise envelope and the carrier amplitude that results in a sudden 2π phase excursion of the carrier-plus-noise vector resultant, R .

Both plus or minus 2π phase excursions can occur with equal probability, which results in a corresponding positive or negative noise spike in the demodulator output.

Using the phasor representation of Figure 3-4, the click event can be defined in terms of a phase excursion of $\pm 2\pi$ radians by the angle ϕ . The probability of such an excursion increases as the input SNR to the discriminator decreases below a value of 10 dB. This figure shows that, for low values of input SNR, a small change in the phase angle between the noise and carrier waveforms can result in a relatively large change in the resultant phase angle.

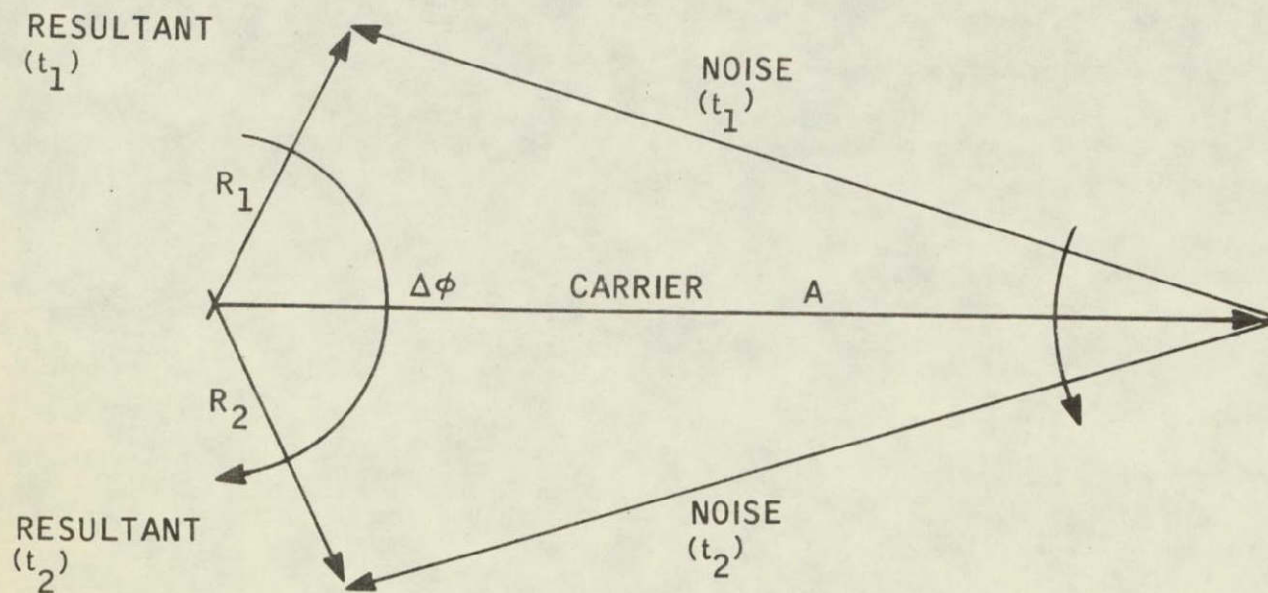


Figure 3-4 Phasor Representation of Noise, Carrier, and Resultant R, Near FM Threshold

3.2 CLICK EVENT (Cont'd)

Since the output of an ideal discriminator is proportional to $d\phi/dt$, the 2π phase excursion causes a noise spike of area 2π to occur at the output as shown in Figure 3-5.

It is also possible for the angle ϕ to experience a phase excursion of 4π , 6π , or even 8π radians. For phase steps exceeding 2π radians, the resulting output noise spike will have a proportionally greater duration prior to postdetection filtering. Figures 3-6 through 3-13 show the click waveform before and after postdetection filtering. Several photographs are provided to illustrate each of the higher order clicks since each unfiltered waveform is unique. Figures 3-6 and 3-7 represent clicks resulting from a $\pm 2\pi$ phase excursion. These noise spikes will be referred to as first order clicks since they are a result of the minimum click-producing phase excursions. Some higher order clicks are also present in these figures, but the clicks referenced in the figure titles are shown in the extreme left portion of the photographs. Figures 3-8 and 3-9 represent second order clicks (4π radians). The duration of the second order clicks is approximately twice that of the first order clicks at the unfiltered output of the demodulator. The noise contribution of the second order clicks is correspondingly greater than that of the first order clicks.

The difference between first and second order clicks can easily be distinguished at the output of the demodulator postdetection filter by observing the relative amplitude of the spikes. The cut-off frequency of the low pass filter determines the duration of the output noise spikes so that both first and second order clicks have the same duration at the filter output. Therefore, the difference in duration between the first and second order clicks at the unfiltered output is translated to an amplitude difference in the filtered output. Table 3-1 summarizes the relative amplitude and duration relationship between the different orders of filtered and unfiltered click waveforms.

Figures 3-10 through 3-13 represent third and fourth order click waveforms at the demodulator output. These higher order clicks occur only for very low values of input SNR, and for practical considerations, their contribution to the total output noise power can be neglected. In most cases the degradation of the demodulator output below threshold will primarily be caused by the occurrence of first order clicks.

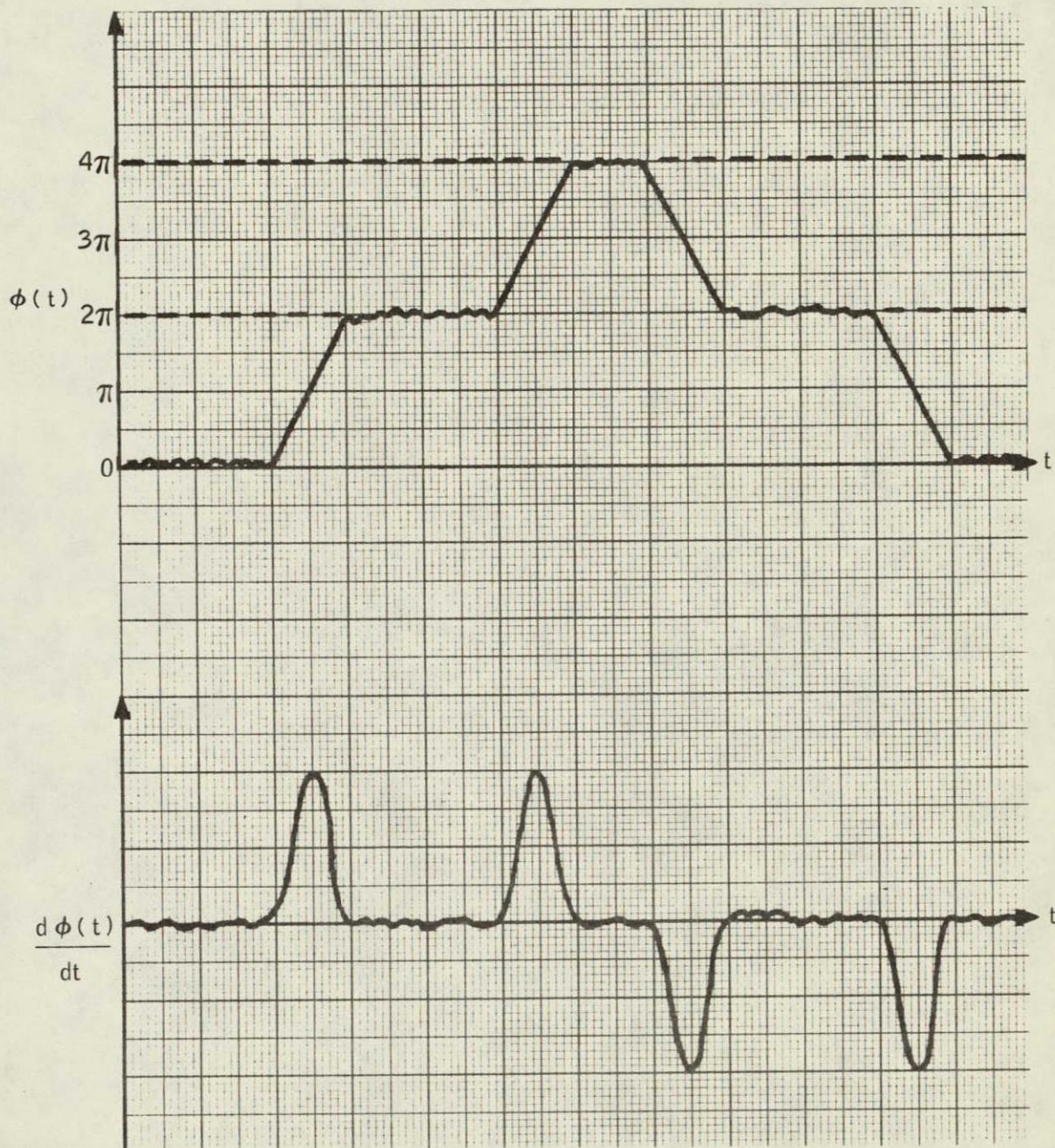


Figure 3-5 Relationship Between $\pm 2\pi$ Phase Excursions and Resulting Impulses of Area 2π

GC10177(A)-9

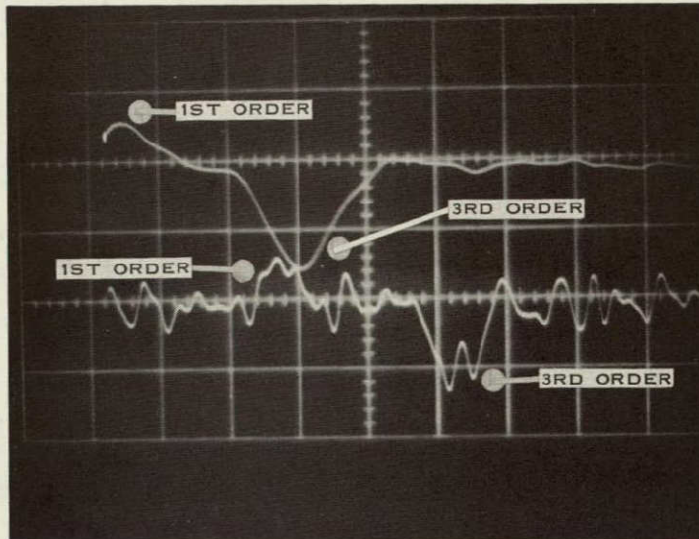


Figure 3-6 First Order Click Waveform
 UPPER TRACE: FILTERED
 LOWER TRACE: UNFILTERED
 HORIZONTAL SCALE: 1 μ SEC/CM

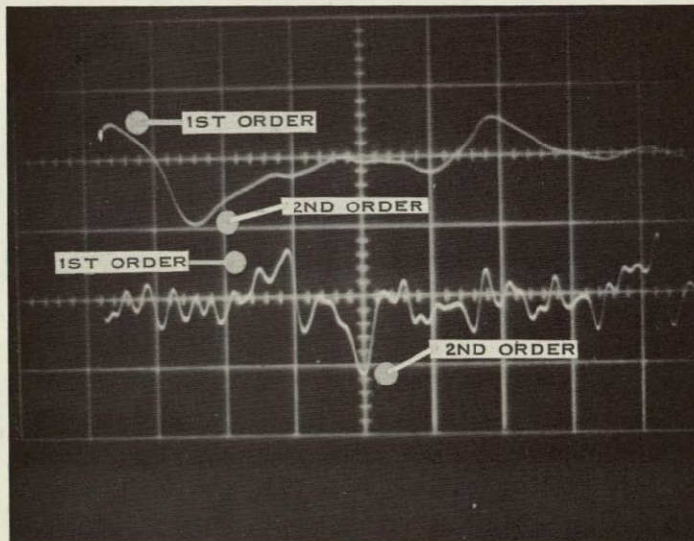


Figure 3-7 First Order Click Waveform
 UPPER TRACE: FILTERED
 LOWER TRACE: UNFILTERED
 HORIZONTAL SCALE: 1 μ SEC/CM

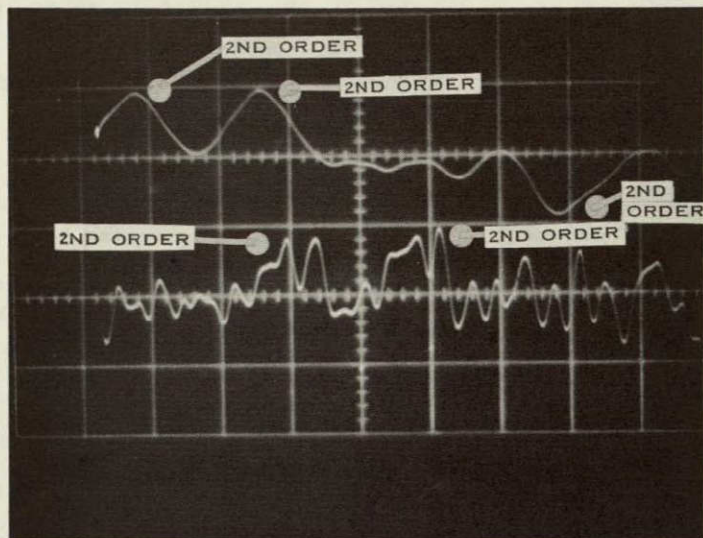


Figure 3-8 Second Order Click Waveform
 UPPER TRACE: FILTERED
 LOWER TRACE: UNFILTERED
 HORIZONTAL SCALE: 1 μ SEC/CM

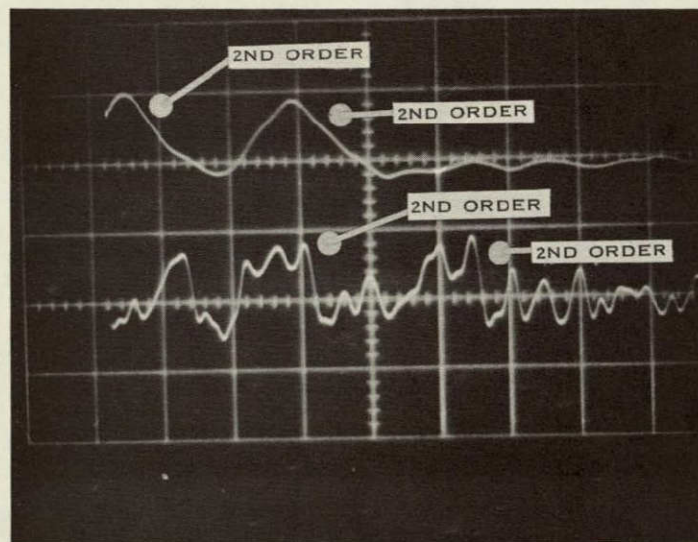


Figure 3-9 Second Order Click Waveform
 UPPER TRACE: FILTERED
 LOWER TRACE: UNFILTERED
 HORIZONTAL SCALE: 1 μ SEC/CM

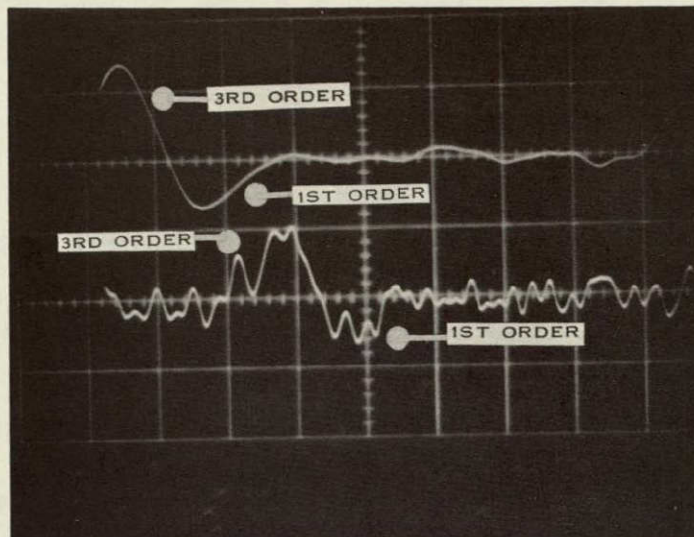


Figure 3-10 Third Order Click Waveform
 UPPER TRACE: FILTERED
 LOWER TRACE: UNFILTERED
 HORIZONTAL SCALE: 1 μ SEC/CM

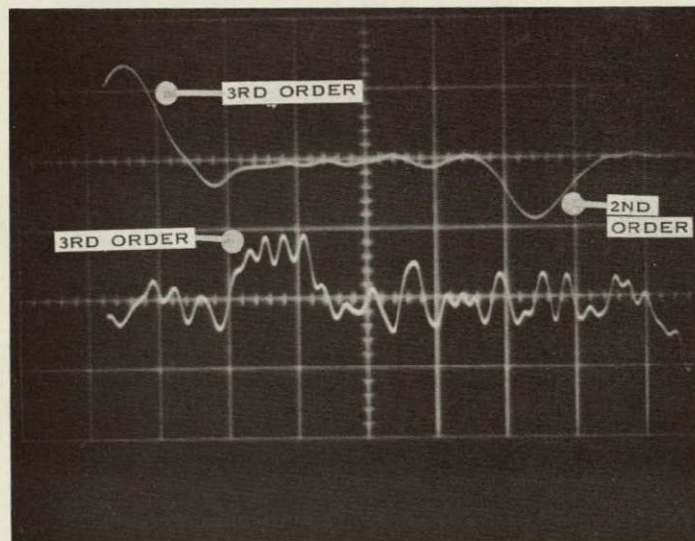


Figure 3-11 Third Order Click Waveform
 UPPER TRACE: FILTERED
 LOWER TRACE: UNFILTERED
 HORIZONTAL SCALE: 1 μ SEC/CM

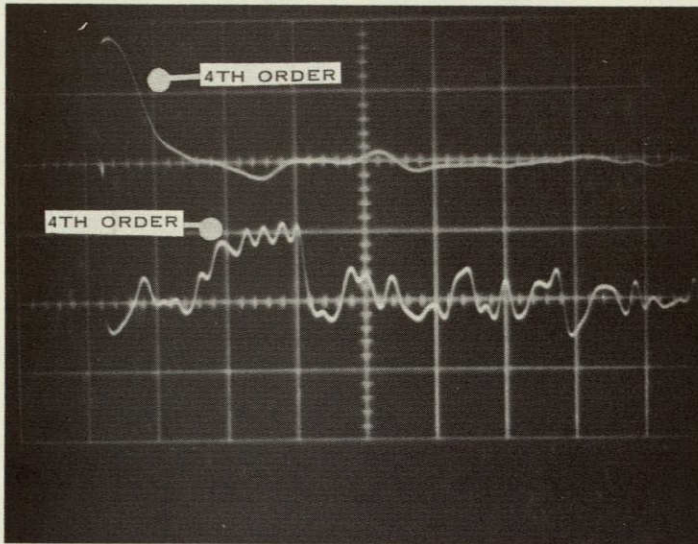


Figure 3-12 Fourth Order Click Waveform
 UPPER TRACE: FILTERED
 LOWER TRACE: UNFILTERED
 HORIZONTAL SCALE: 1 μ SEC/CM

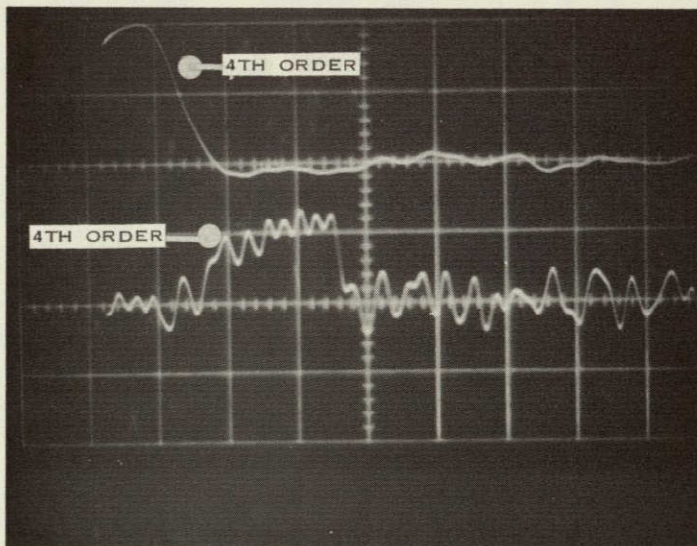


Figure 3-13 Fourth Order Click Waveform
 UPPER TRACE: FILTERED
 LOWER TRACE: UNFILTERED
 HORIZONTAL SCALE: 1 μ SEC/CM

TABLE 3-1

DURATION AND AMPLITUDE
CHARACTERISTICS OF Nth ORDER CLICK WAVEFORMS

CLICK ORDER	UNFILTERED DURATION (10^{-6} SEC)	FILTERED RELATIVE AMPLITUDE (CM)
FIRST	0 5	0 5
SECOND	1 0	1 0
THIRD	1 5	1 5
FOURTH	2 0	2 0

3.3 FM DEMODULATOR PERFORMANCE WITH CLICK NOISE

The click event was described in Paragraph 3.2 in terms of the interaction between an unmodulated carrier and a quadrature-carrier representation of the input narrow-band noise. However, in order to discuss the effect of click noise on the performance of an FM demodulator, it is necessary to consider a modulated input signal.

An FM signal can be represented by $S(t)$ in the following form

$$S(t) = A \cos [\omega_c t + \phi(t)], \quad (7)$$

where A is a constant representing the amplitude of the signal, $\omega_c = 2\pi f_c$, which is the carrier angular frequency, and $\phi(t)$ is the modulation term

The modulation information can be utilized to determine the instantaneous frequency of the carrier in the following manner

$$\omega_1 = \omega_c + \frac{d\phi}{dt} = \omega_c + \Delta\omega m(t) \quad (8)$$

where ω_1 is the instantaneous frequency of the carrier, ω_c is the carrier rest frequency when modulation is not present, and $\Delta\omega$ is the carrier frequency deviation, and $m(t)$ is the modulating signal waveform

The magnitude of the frequency deviation $\Delta\omega$ is determined by the amplitude of the modulating waveform $m(t)$ and by the sensitivity of the transmitter modulator

For sinusoidal modulation, equation (8) can be written as follows

$$\omega_1 = \omega_c + \Delta\omega \cos \omega_m t \quad (9)$$

3 3 FM DEMODULATOR PERFORMANCE WITH CLICK NOISE (Cont'd)

Since
$$\Delta\omega \cos \omega_m t = \frac{d\phi}{dt}$$

Then
$$\phi = \int \Delta\omega \cos \omega_m t dt \quad (10)$$

Therefore, equation (7) can be rewritten as

$$\begin{aligned} S(t) &= A \cos \left[\omega_c t + \int \Delta\omega \cos \omega_m t dt \right] \\ &= A \cos \left[\omega_c t + \frac{\Delta\omega}{\omega_m} \sin \omega_m t \right] \end{aligned} \quad (11)$$

By definition, $\frac{\Delta\omega}{\omega_m}$ is designated as the modulation index, β

The final form of equation (1) is

$$S(t) = A \cos \left[\omega_c t + \beta \sin \omega_m t \right] \quad (12)$$

The input SNR to the demodulator is determined by considering a rectangular predetection bandpass filter having a bandwidth

$$BW_{IF} = 2(\Delta f + f_m) \quad , \quad (13)$$

where Δf is the peak frequency deviation and f_m is the modulating frequency

The input signal power can be found from equation (12) to be

$$S_1 = \frac{A^2}{2} \quad (14)$$

3.3 FM DEMODULATOR PERFORMANCE WITH CLICK NOISE (Cont'd)

and the input noise power is

$$N_1 = KT BW_{IF} \quad , \quad (15)$$

where K is Boltzman's constant (1.38×10^{-23} Watts-sec $^{\circ}K^{-1}$), T is the effective system temperature in degrees Kelvin, and BW_{IF} is defined by equation (13)

Therefore, the input SNR can be found by dividing equation (14) by equation (15)

$$S_1/N_1 = \frac{A^2}{2KT BW_{IF}} \quad (16)$$

The output signal power at high levels of input SNR is independent of the input carrier amplitude A and is a function of the frequency deviation Δf

$$S_o = K_D \frac{\Delta\omega^2}{2} = K_D \frac{(2\pi\Delta f)^2}{2} \quad (17)$$

The output noise power of the discriminator for the unmodulated case can be determined by considering the noise disturbance about the carrier frequency ω_c . The input noise can be represented in quadrature form by the following expression

$$N_{\omega_1} = X(t) \cos \omega_c t = Y(t) \sin \omega_c t \quad (18)$$

where $X(t)$ and $Y(t)$ represent the in-phase and quadrature components of noise and are defined by a summation of Gaussian random variables having zero mean.

$$\overline{X(t)} = \overline{Y(t)} = 0 \quad (19)$$

and

$$\overline{X^2(t)} = \overline{Y^2(t)} = N_{\omega_c}^2 \quad (20)$$

3 3 FM DEMODULATOR PERFORMANCE WITH CLICK NOISE (Cont'd)

By definition³,

$$X(t) = \sum_{n=1}^{\infty} \left[x_n \cos(n\omega_o - \omega_c)t + y_n \sin(n\omega_o - \omega_c)t \right] \quad (21)$$

$$Y(t) = \sum_{n=1}^{\infty} \left[x_n \sin(n\omega_o - \omega_c)t - y_n \cos(n\omega_o - \omega_c)t \right] \quad (22)$$

where x_n and y_n are Gaussian random variables with zero mean. The total expression for the instantaneous carrier plus noise can be written as follows

$$\begin{aligned} \text{Total input voltage} &= A \cos \omega_c t + X(t) \cos \omega_c t + Y(t) \sin \omega_c t \\ &= [A+X(t)] \cos \omega_c t + Y(t) \sin \omega_c t \end{aligned} \quad (23)$$

The phase error caused by the noise disturbance about the carrier frequency ω_c is represented by ϕ_e

$$\phi_e = \tan^{-1} \frac{Y(t)}{A+X(t)} \approx \frac{Y(t)}{A} \quad (24)$$

This expression is similar to equation (6) for the angle ϕ

Similarly, the frequency error, or noise disturbance about the carrier frequency ω_c , at the output of the discriminator is represented by ω_e

$$\dot{\phi}_e = \omega_e \approx \frac{\dot{Y}(t)}{A} \quad (25)$$

Substituting equation (22) for $Y(t)$ into equation (25), we get

$$\omega_e = \frac{1}{A} \frac{d}{dt} \sum_{n=1}^{\infty} \left[x_n \sin(n\omega_o - \omega_c)t - y_n \cos(n\omega_o - \omega_c)t \right] \quad (26)$$

³ John J. Downing, *Modulation Systems and Noise* (Englewood Cliffs, 1964), p.52

3.3 FM DEMODULATOR PERFORMANCE WITH CLICK NOISE (Cont'd)

$$\omega_e = \frac{1}{A} \sum_{n=1}^{\infty} \left[x_n (n\omega_o - \omega_c) \cos (n\omega_o - \omega_c) t + y_n (n\omega_o - \omega_c) \sin (n\omega_o - \omega_c) t \right] \quad (27)$$

$$\omega_e = \frac{2\pi}{A} \left[\sum_{n=1}^{\infty} \left[x_n (nf_o - f_c) \cos (n\omega_o - \omega_c) t + y_n (nf_o - f_c) \sin (n\omega_o - \omega_c) t \right] \right] \quad (28)$$

The average output noise power is proportional to $\overline{\omega_e^2}$

$$\overline{\omega_e^2} = \frac{4\pi^2}{A^2} \sum_{n=1}^{\infty} \left[\overline{x_n^2 (nf_o - f_c)^2 \cos^2 (n\omega_o - \omega_c) t + y_n^2 (nf_o - f_c)^2 \sin^2 (n\omega_o - \omega_c) t} \right. \\ \left. + \overline{2x_n y_n (nf_o - f_c)^2 \cos (n\omega_o - \omega_c) t \sin (n\omega_o - \omega_c) t} \right] \quad (29)$$

Since the mean value of the cross product term,

$$2x_n y_n (nf_o - f_c)^2 \cos (n\omega_o - \omega_c) t \sin (n\omega_o - \omega_c) t,$$

is zero,

$$\overline{\omega_e^2} = \frac{4\pi^2}{A^2} \sum_{n=1}^{\infty} (nf_o - f_c)^2 \left[\overline{x_n^2 \cos^2 (n\omega_o - \omega_c) t} + \overline{y_n^2 \sin^2 (n\omega_o - \omega_c) t} \right] \quad (30)$$

but, $\overline{x_n} = \overline{y_n} = 0$ (31)

and $\overline{x_n^2} = \overline{y_n^2} = \frac{KT}{\tau}$ (32)

Where KT = equivalent noise spectral density and τ is the period of noise under consideration

3.3 FM DEMODULATOR PERFORMANCE WITH CLICK NOISE (Cont'd)

Therefore,

$$\overline{\omega_e^2} = \frac{4\pi^2}{A^2} \sum_{n=1}^{\infty} \frac{KT}{\tau} (nf_o - f_c)^2 \left[\cos^2(n\omega_o - \omega_c)t + \sin^2(n\omega_o - \omega_c)t \right] \quad (33)$$

Since $\left[\cos^2(n\omega_o - \omega_c)t + \sin^2(n\omega_o - \omega_c)t \right] = 1$ we have,

$$\overline{\omega_e^2} = \frac{4\pi^2}{A^2} \sum_{n=1}^{\infty} \frac{KT}{\tau} (nf_o - f_c)^2 \quad (34)$$

By making the period τ relatively long, the summation can be changed to an integral in equation (34).

$$\overline{\omega_e^2} = \frac{4\pi^2}{A^2} \int_{f_c - f_m}^{f_c + f_m} KT (f_o - f_c)^2 df_o \quad (35)$$

where f_m is the maximum modulating frequency (the cutoff frequency of the postdetection low pass filter, BW_o)

$$\begin{aligned} \overline{\omega_e^2} &= 4\pi^2 \left(\frac{KT}{A^2} \right) \left[\frac{(f_o - f_c)^3}{3} \right] \Bigg|_{f_o = f_c - f_m}^{f_o = f_c + f_m} \\ &= 4\pi^2 \left(\frac{KT}{3A^2} \right) \left[\left(f_c + f_m - f_c \right)^3 - \left(f_c - f_m - f_c \right)^3 \right] \\ &= 4\pi^2 \left(\frac{KT}{3A^2} \right) \left[f_m^3 + f_m^3 \right] = \frac{8\pi^2 f_m^3 KT}{3A^2} \quad (36) \end{aligned}$$

3.3 FM DEMODULATOR PERFORMANCE WITH CLICK NOISE (Cont'd)

Finally, we get

$$N_o = K_D \omega_e^2 = \frac{2KT(f_m)^3 4\pi^2 K_D}{3A^2} \quad (37)$$

The output SNR can be found by dividing equation (17) by equation (37).

$$S_o/N_o = \frac{3\Delta f^2 A^2}{4KTf_m^3} \quad (38)$$

The output SNR can be expressed in terms of the input SNR by combining equation (16) and equation (38)

$$S_o/N_o = \left(S_1/N_1 \right) \frac{3\Delta f^2 BW_{IF}}{2f_m^3} \quad (39)$$

By assuming that the cutoff frequency of the postdetection filter is the same as the maximum modulating frequency f_m we can rewrite equation (39) as follows

$$S_o/N_o = \left(S_1/N_1 \right) \frac{3\Delta f^2 BW_{IF}}{2BW_o^3} \quad (40)$$

where BW_o is the bandwidth of the postdetection low pass filter

3 3 FM DEMODULATOR PERFORMANCE WITH CLICK NOISE (Cont'd)

Remembering that the modulation index β is defined as

$$\beta \equiv \frac{\Delta\omega}{\omega} = \frac{2\pi\Delta f}{2\pi f_m} = \frac{\Delta f}{BW_o}$$

we can express equation (39) another way

$$S_o/N_o = \left(S_1/N_1 \right) \frac{3\beta^2 BW_{IF}}{2BW_o} \quad (41)$$

Equations (39), (40), and (41) express the SNR transfer characteristic of an FM discriminator operating in the linear region above threshold. This region corresponds to the portion of the curve (see Figure 3-1) for values of input SNR greater than 10 dB.

The output noise represented by equation (37) has a Gaussian distribution and a parabolic spectrum. This noise determines the behavior of the SNR transfer curve in the linear region above threshold. The occurrence of click noise in the output, however, causes the transfer curve to deviate from its linearity, and the FM threshold effect results. Therefore, equations (39), (40) and (41) are valid only at values of input SNR that are large enough (generally > 10 dB) such that noise clicks do not appear in the output.

In order to describe the performance of an FM discriminator for values of input SNR below 10 dB, it is necessary to consider the addition of click noise to the Gaussian component in the output.

The noise power contribution of click noise increases as the number of clicks per second increases.

3.3 FM DEMODULATOR PERFORMANCE WITH CLICK NOISE (Cont'd)

Following the analysis of S O Rice⁴, the output noise power below threshold can be found by adding the contributions of the Gaussian and click noise as shown below

$$N'_o = N_o + N_c \quad (42)$$

where N'_o is the total output noise power, N_o is the Gaussian noise contribution, and N_c is the click noise contribution

Rearranging equation (39), we get

$$N_o = \frac{2S_o f_m^3}{\left(\frac{S_1}{N_1}\right)^2 3\Delta f^2 BW_{IF}} \quad (43)$$

Substituting equation (17) into equation (43), we have

$$N_o = \frac{K_D 4\pi^2 \Delta f^2 f_m^3}{\left(\frac{S_1}{N_1}\right)^2 3\Delta f^2 BW_{IF}} = \frac{K_D 4\pi^2 f_m^3}{3BW_{IF} \left(\frac{S_1}{N_1}\right)} \quad (44)$$

The noise power contribution of click noise N_c has been found by Rice to be $8\pi^2(N^+ + N^-)f_m$

$$N_c = K_D 8\pi^2(N^+ + N^-)f_m \quad (45)$$

where N^+ and N^- represent the number of positive and negative clicks per second, respectively

⁴Rice, pp 375-424

3 3 FM DEMODULATOR PERFORMANCE WITH CLICK NOISE (Cont'd)

Rice further shows that the expression for the click rate N^+ is given by

$$N^+ = \frac{r}{2} \left(1 - \text{erf} \sqrt{S_1/N_1} \right) \quad (46)$$

where r is defined as the radius of gyration of the power spectrum $\omega_e(f)$ about its axis of symmetry, $f = f_c$

$$r = \frac{1}{2\pi} \left[\frac{(2\pi)^2 \int_0^{\infty} (f-f_c)^2 \omega(f) df}{\int_0^{\infty} \omega(f) df} \right]^{1/2} \quad (47)$$

$$r = \frac{1}{2\pi} \left[\frac{\pi^2 \omega_o BW_{IF}^3}{3\omega_o BW_{IF}} \right]^{1/2} = \frac{BW_{IF}}{2\sqrt{3}} \quad (48)$$

Substituting equation (48) into equation (46) we obtain

$$N^+ = \frac{BW_{IF}}{4\sqrt{3}} \left(1 - \text{erf} \sqrt{S_1/N_1} \right) \quad (49)$$

The click rate given by equation (49) is valid only for an unmodulated carrier. Assuming that the number of positive and negative clicks are equal, then equation (45) can be written as

$$N_c = K_D 16\pi^2 (N^+)^2 f_m \quad (50)$$

3 3 FM DEMODULATOR PERFORMANCE WITH CLICK NOISE (Cont'd)

Substituting equation (49) into equation (50) we get

$$N_c = \frac{K_D 4\pi^2 BW_{IF}}{\sqrt{3}} \left(1 - \text{erf} \sqrt{S_1/N_1} \right) f_m \quad (51)$$

Therefore, the total average output noise power can be written as

$$N_o' = N_o + N_c = \frac{4\pi^2 f_m^3 K_D}{3BW_{IF} \left(S_1/N_1 \right)} + \frac{K_D f_m 4\pi^2 BW_{IF}}{\sqrt{3}} \left(1 - \text{erf} \sqrt{S_1/N_1} \right) \quad (52)$$

From equation (17) we get,

$$S_o = \frac{K_D (2\pi\Delta f)^2}{2} \quad (53)$$

Dividing equation (53) by equation (52), we obtain the following expression for the SNR transfer characteristic of an FM discriminator

$$S_o/N_o' = \frac{2\pi^2 \Delta f^2}{\frac{4\pi^2 f_m^3}{3BW_{IF} \left(S_1/N_1 \right)} \left[1 + \frac{3BW_{IF}^2 \left(S_1/N_1 \right)}{\sqrt{3} f_m^2} \left(1 - \text{erf} \sqrt{S_1/N_1} \right) \right]} \quad (54)$$

Substituting BW_o in equation (54) for f_m and rearranging, we obtain

$$S_o/N_o' = \frac{3/2 \left[\frac{(\Delta f^2) BW_{IF} \left(S_1/N_1 \right)}{BW_o^3} \right]}{\sqrt{3} \left(\frac{BW_{IF}}{BW_o} \right)^2 \left(S_1/N_1 \right) \left(1 - \text{erf} \sqrt{S_1/N_1} \right) + 1} \quad (55)$$

Equation (55) can be expressed in the following form by substituting β for $\frac{\Delta f}{BW_o}$

3 3 FM DEMODULATOR PERFORMANCE WITH CLICK NOISE (Cont'd)

$$S_o/N_o = \frac{3/2 (\beta^2) \left(\frac{BW_{IF}}{BW_o}\right) \left(S_1/N_1\right)}{\sqrt{3} \left(\frac{BW_{IF}}{BW_o}\right)^2 \left(\frac{S_1}{N_1}\right) \left(1 - \text{erf} \sqrt{S_1/N_1}\right) + 1} \quad (56)$$

Plotting equation (56) gives results similar to the curve shown in Figure 3-1. The deviation from the linear portion of the curve is due to the click noise contribution as expressed by equation (51). For values of input SNR greater than 10 dB, the click noise term becomes negligible, and equation (56) reduces to the form of equation (41).

It should be noted that the click noise term expressed by equation (51) is valid only for an unmodulated carrier at the input to the discriminator. For a modulated signal, the click rate increases substantially so that the portion of the curve below threshold in Figure 3-1 exhibits a more severe slope.

The previous analysis indicates that the threshold effect in an FM system is primarily determined by the click rate in the demodulator output. This implies that a substantial extension of threshold could be accomplished by reducing the click rate at the output for a given input SNR. Experimental results have verified that, indeed, the threshold performance of an FM demodulator can be improved by reducing click noise. The following sections describe a threshold extension technique that is based on the detection and elimination of click noise in the demodulator output.

3 4 CLICK SYMMETRY

For a properly aligned FM demodulator, both the positive and negative noise spikes in the output below threshold are present in equal quantity. However, certain conditions can exist that cause the output noise voltage to be unsymmetrical as represented by the predominance of either positive or negative clicks.

The most common cause of unsymmetrical click noise is an input carrier that is not centered properly in the passband of the demodulator predetection filter. Either a frequency drift in the transmitter or an unaligned predetection filter can result in offsets that cause unsymmetrical clicks. The effect of unsymmetrical clicks is to increase the output noise power and, hence, degrade the performance of the demodulator. Figure 3-14 illustrates the effect of input frequency offsets on the output noise power, while Figure 3-15 represents measured data that shows the output noise power increase as a function of carrier offsets.

The problem of unsymmetrical click noise is significant since the CSM FM transmitter can experience offsets of ± 500 KHz from center frequency which adversely affects the performance of the FM channels.

The amount of degradation is a function of frequency offset, input SNR, and the shape of the filter response. In most cases a degradation of 1 dB to 2 dB was measured in tests of the CSM modes using offsets of ± 500 KHz. The problem of frequency offsets can be solved by implementing Automatic Frequency Control (AFC) in the MSFN receiver so that the IF frequency is always centered in the predetection filter passband. It is also necessary to use a predetection filter that has a symmetrical frequency response.

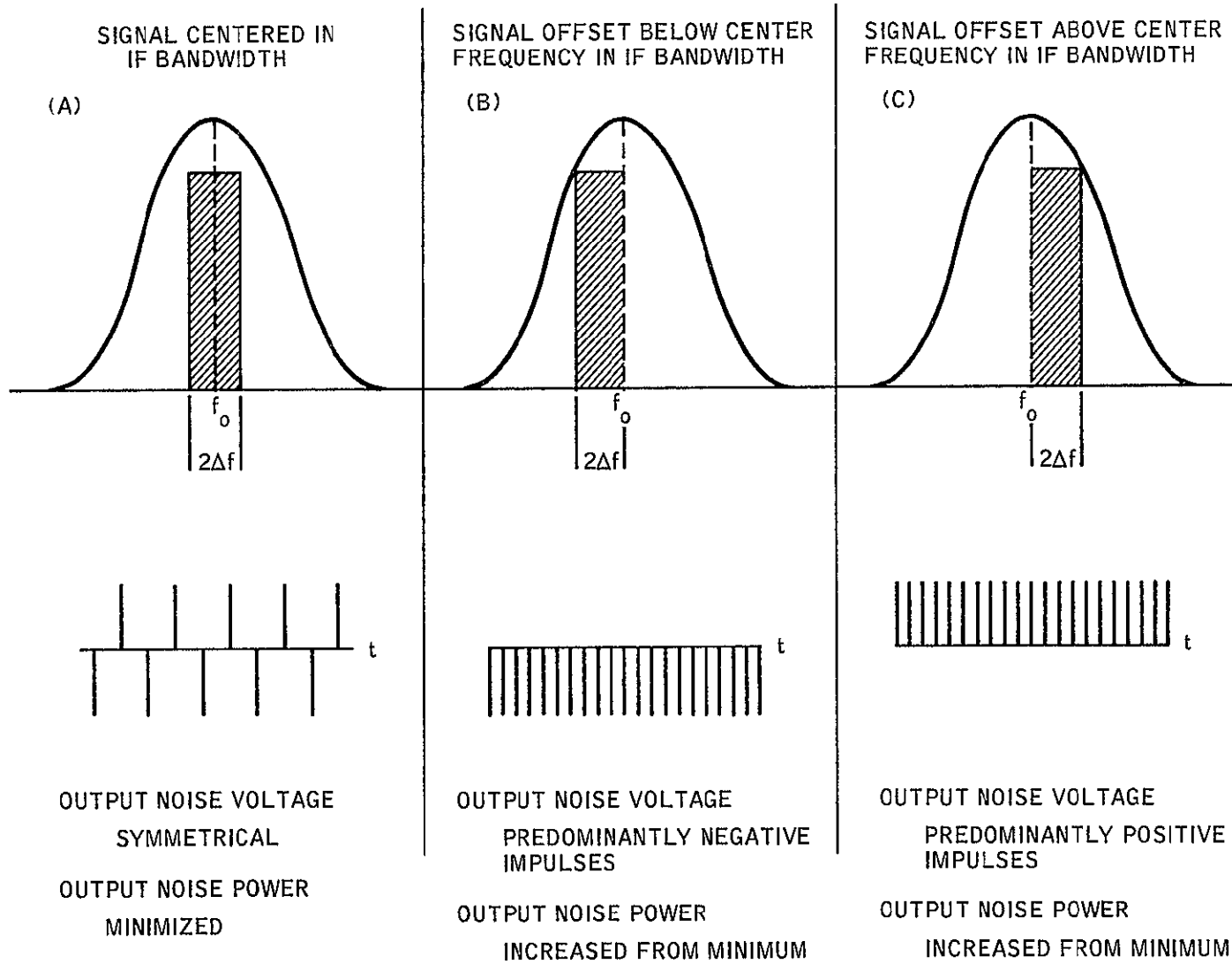
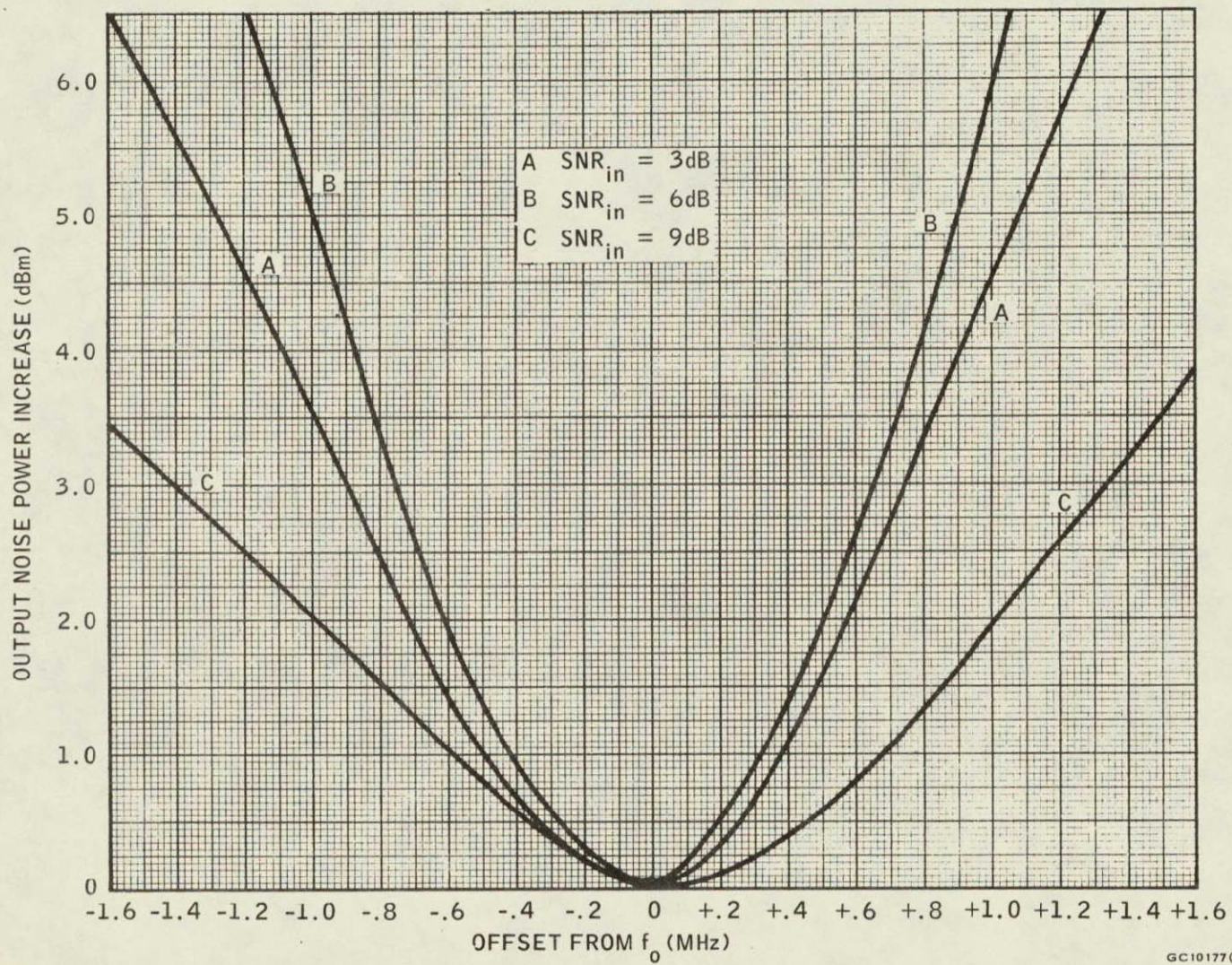


Figure 3-14 Effect of Carrier Offset on Click Noise Distribution



GC10177(A)-6

Figure 3-15 Output Noise Power Increase vs Center Frequency Offset

SECTION 4

THRESHOLD EXTENSION TECHNIQUES

4.1 GENERAL

The discussion of FM threshold in the preceding section recognized the presence of high amplitude impulse noise (click noise) in the demodulator output as a primary factor contributing to the occurrence of threshold in an FM system.

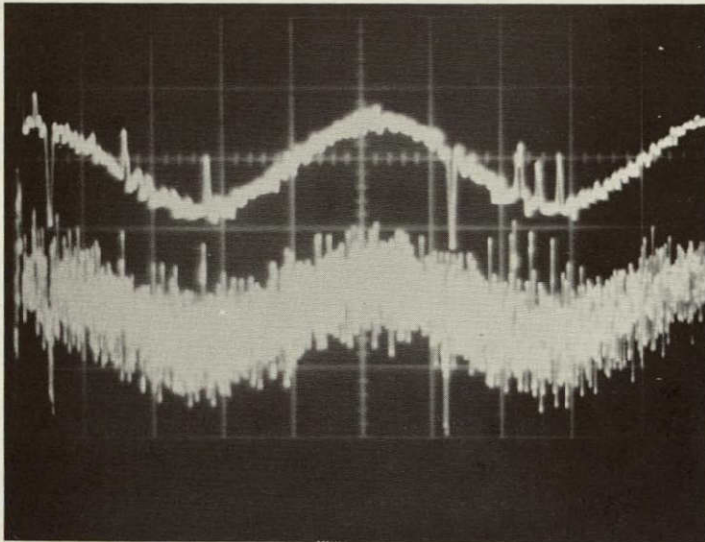
Certain distinguishing characteristics of click noise provide a basis for practical techniques which can be implemented at the output of an FM demodulator to extend the threshold performance of the system. The threshold extension technique that will be described in this section is based on the accomplishment of the following two steps:

- A. Detection of the click producing noise impulses in the demodulator output by distinguishing them from the demodulated signal and low-level Gaussian noise.
- B. Utilization of the detected click noise information to perform a click elimination operation on a delayed version of the demodulator output.

4.2 CLICK DETECTION

The problem of click detection can be simplified by observing that, in most cases, the peak amplitude of the click-producing impulse noise is greater than that of both the modulation and Gaussian noise in the unfiltered demodulator output. Figures 4-1 through 4-6 are presented to illustrate this point.

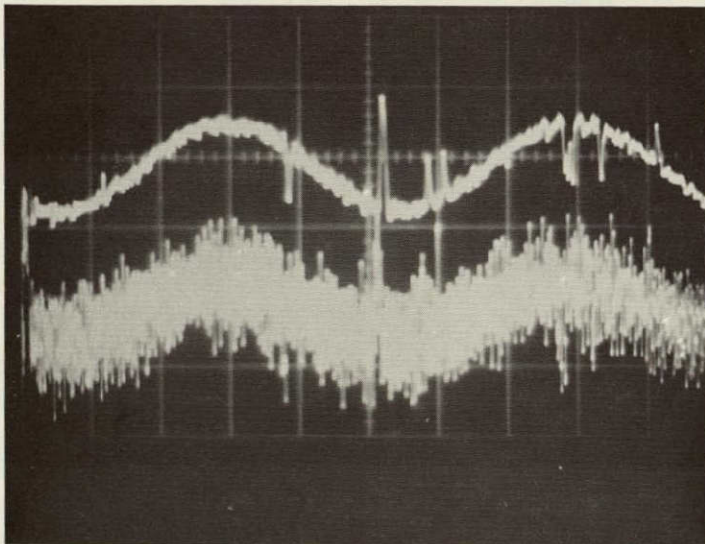
The upper waveform in each photograph represents the signal plus noise output of a 500 KHz low-pass postdetection filter whereas the lower sweep in each figure represents the signal plus noise present in the unfiltered demodulator output. The sweeps in each photograph are aligned such that the relationship between unfiltered



$f_m = 10 \text{ KHz}$
 $\Delta f = 1 \text{ MHz}$
 $BW_o = 500 \text{ KHz}$

Figure 4-1 Demodulated Signal Plus Noise Waveform With and Without Postdetection Filtering ($f_m = 10 \text{ KHz}$)

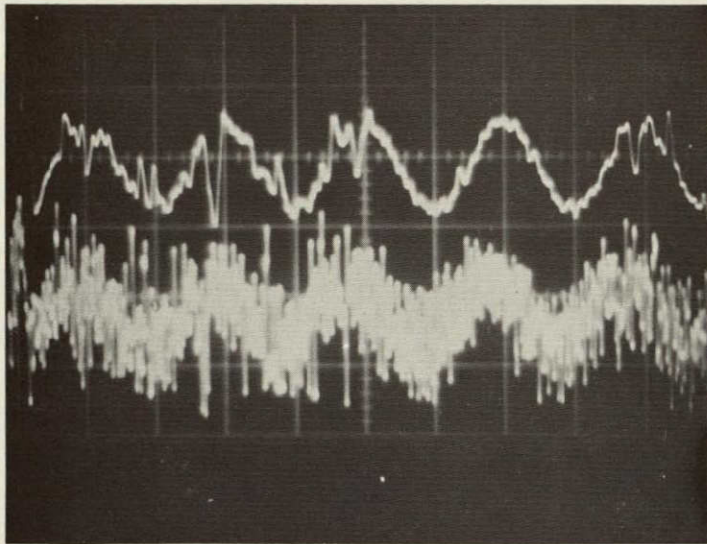
UPPER TRACE: FILTERED
 LOWER TRACE: UNFILTERED
 HORIZONTAL SCALE: $20 \mu\text{SEC/CM}$



$f_m = 10 \text{ KHz}$
 $\Delta f = 1 \text{ MHz}$
 $BW_o = 500 \text{ KHz}$

Figure 4-2 Demodulated Signal Plus Noise Waveform with and Without Postdetection Filtering ($f_m = 10 \text{ KHz}$)

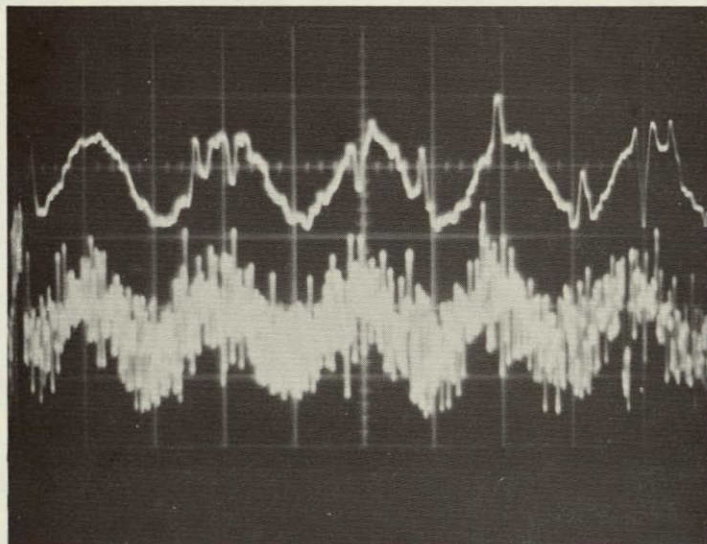
UPPER TRACE: FILTERED
 LOWER TRACE: UNFILTERED
 HORIZONTAL SCALE: $20 \mu\text{SEC/CM}$



$f_m = 50 \text{ KHz}$
 $\Delta f = 1 \text{ MHz}$
 $BW_o = 500 \text{ KHz}$

Figure 4-3 Demodulated Signal Plus Noise Waveform With and Without Postdetection Filtering ($f_m = 50 \text{ KHz}$)

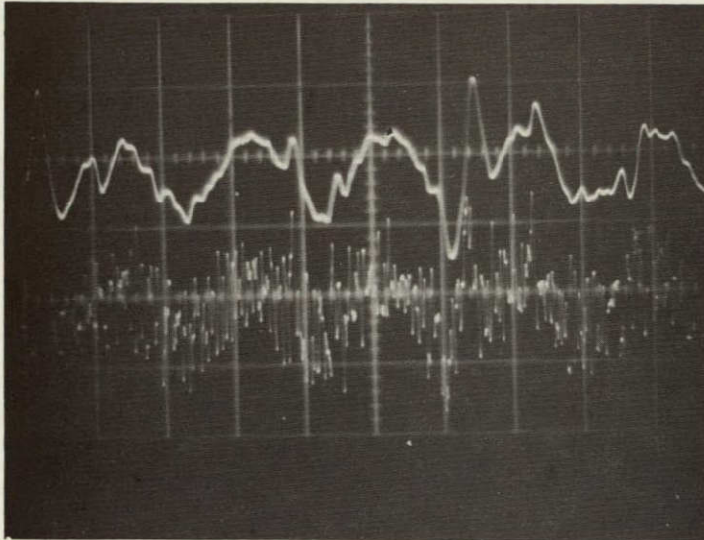
UPPER TRACE: FILTERED
 LOWER TRACE: UNFILTERED
 HORIZONTAL SCALE: $10 \mu\text{SEC/CM}$



$f_m = 50 \text{ KHz}$
 $\Delta f = 1 \text{ MHz}$
 $BW_o = 500 \text{ KHz}$

Figure 4-4 Demodulated Signal Plus Noise Waveform With and Without Postdetection Filtering ($f_m = 50 \text{ KHz}$)

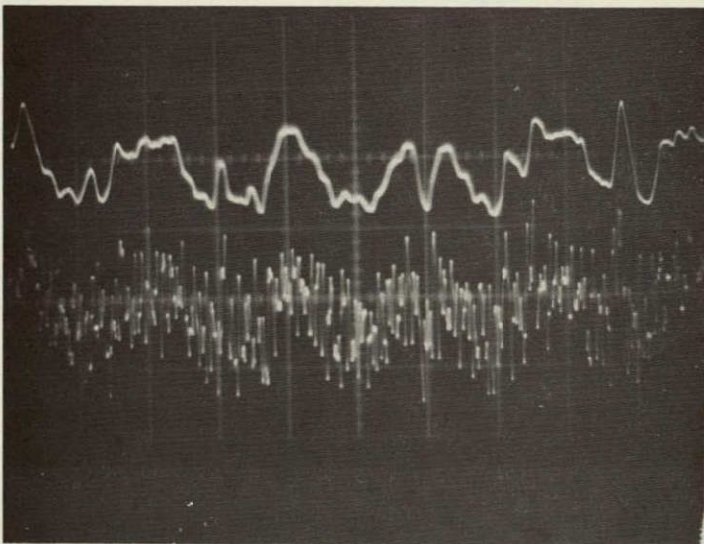
UPPER TRACE: FILTERED
 LOWER TRACE: UNFILTERED
 HORIZONTAL SCALE: $10 \mu\text{SEC/CM}$



$f_m = 100 \text{ KHz}$
 $\Delta f = 1 \text{ MHz}$
 $BW_0 = 500 \text{ KHz}$

Figure 4-5 Demodulated Signal Plus Noise Waveform With and Without Postdetection Filtering ($f_m = 100 \text{ KHz}$)

UPPER TRACE: FILTERED
 LOWER TRACE: UNFILTERED
 HORIZONTAL SCALE: $5 \mu\text{SEC/CM}$



$f_m = 100 \text{ KHz}$
 $\Delta f = 1 \text{ MHz}$
 $BW_0 = 500 \text{ KHz}$

Figure 4-6 Demodulated Signal Plus Noise Waveform With and Without Postdetection Filtering ($f_m = 100 \text{ KHz}$)

UPPER TRACE: FILTERED
 LOWER TRACE: UNFILTERED
 HORIZONTAL SCALE: $5 \mu\text{SEC/CM}$

4 2 CLICK DETECTION (Cont'd)

and filtered waveforms may be observed for a particular click event. It should be noted that the 500 KHz postdetection filter acts to attenuate (as well as to broaden) the click waveform.

It is important to note that a click occurs on the 500 KHz low-pass filtered output only when the peak amplitude of the corresponding noise impulse in the unfiltered output exceeds the average peak amplitude of the modulation plus Gaussian noise. There are, however, a certain number of high amplitude noise impulses present on the unfiltered waveforms shown in Figures 4-1 through 4-6 that reach the amplitude of the click-producing noise spikes but do not result in a corresponding click on the unfiltered output waveform. These noise spikes belong to the Gaussian portion of the unfiltered output noise whose energy is concentrated primarily in frequencies above the 500 KHz cutoff of the low-pass postdetection filter. The parabolic spectrum of these occasional high amplitude excursions of the Gaussian noise do not produce clicks on the filtered output waveform since most of the energy is concentrated in frequencies above the cutoff frequency of the low-pass postdetection filter.

The probability of detecting these non-click-producing noise impulses can be minimized by implementing a pre-click detection filter to attenuate the higher frequency Gaussian noise components. The relative high amplitude characteristic of the click-producing impulse noise will be preserved if the cutoff frequency of the filter is high compared with the 500 KHz postdetection filter. A 2 MHz low-pass filter was used for this purpose as shown in Figure 4-7.

Experimental results have shown that amplitude detection of the unfiltered click noise in the demodulator output is a simple and efficient means for obtaining the desired information indicating the occurrence of a click. The actual detection process is accomplished with a pair of conventional Schmidt triggers. It is necessary to use two triggers since both positive and negative clicks must be independently detected.

These devices are configured to detect noise spikes that exceed a predetermined positive or negative voltage level. The reference (trigger) voltage level is selected so that only the click-producing noise spikes will be detected. Figure 4-7 shows the system configuration for the click detection process.

The output of the amplitude level detector is used to trigger a pulse generator which provides gating pulses for the click elimination circuitry.

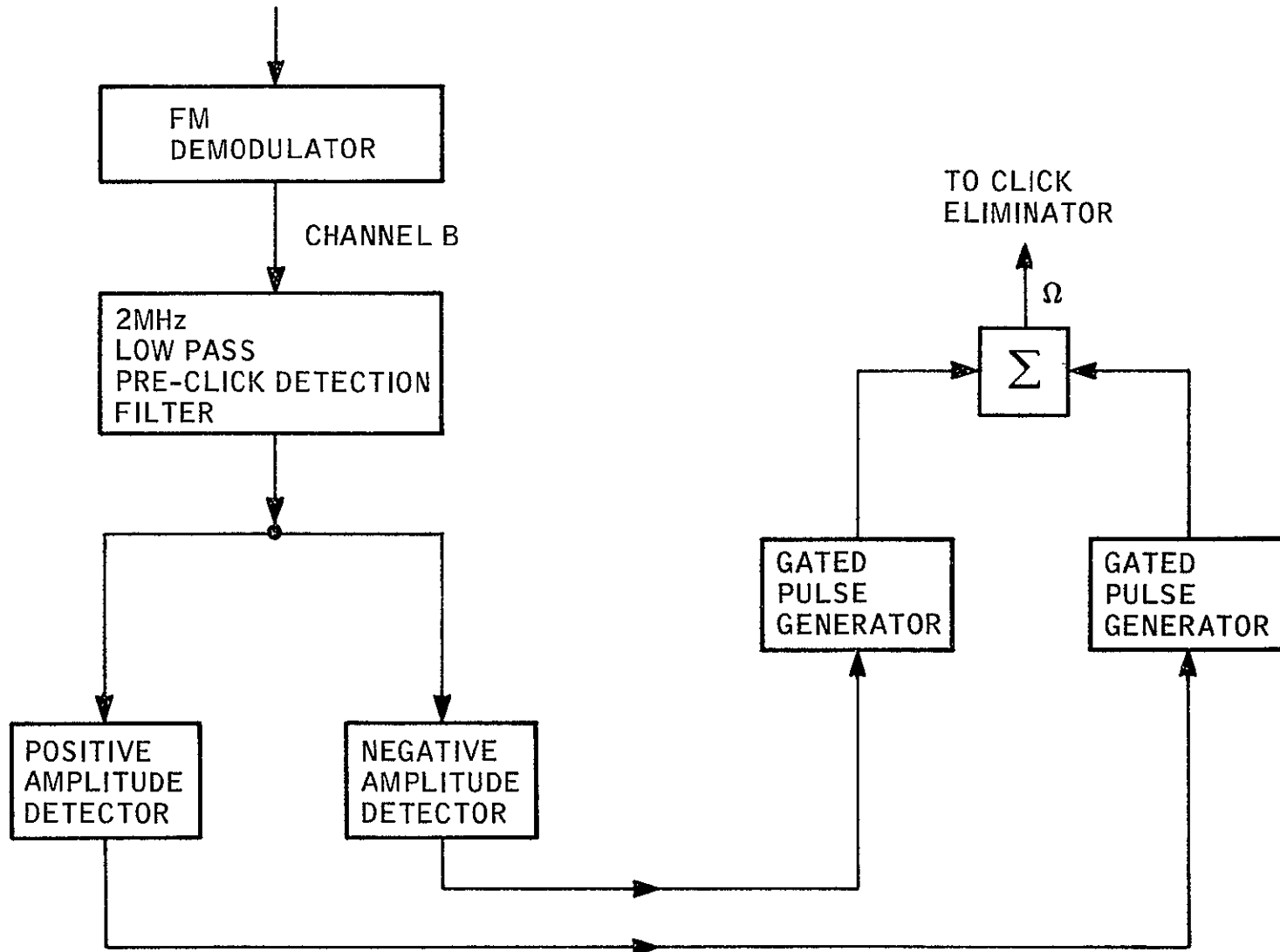


Figure 4-7 Click Detector Block Diagram

4.3 CLICK ELIMINATION

The detected click information is used to perform a click elimination operation on a delayed version of the demodulator output. The elimination process is accomplished by first passing the delayed demodulator output through an amplifier whose output can be gated off for a predetermined time.

Gating pulses from the click detection system are then supplied to the amplifier so that it is turned off at the beginning of a click event. The turnoff time of the amplifier is preset to coincide with the duration of the click.

A "holding" circuit is used in conjunction with the amplifier to provide a constant output voltage from the system during the time that the amplifier is biased off. The output voltage of the "holding" circuit corresponds to the amplitude of the demodulator output just before the beginning of the click. The net effect of the click elimination circuitry is to provide an estimate of the modulation as a substitute for the high amplitude noise spike in the demodulated output. A block diagram of the click elimination system is shown in Figure 4-8.

Since the click elimination process is performed prior to postdetection filtering, the turnoff time, or click duration, is small compared with the average modulation frequency. The 500 KHz postdetection filter provides a smoothing effect on the click-eliminated output, which enhances the performance of the device.

A block diagram of the complete threshold extension device is shown in Figure 4-9.

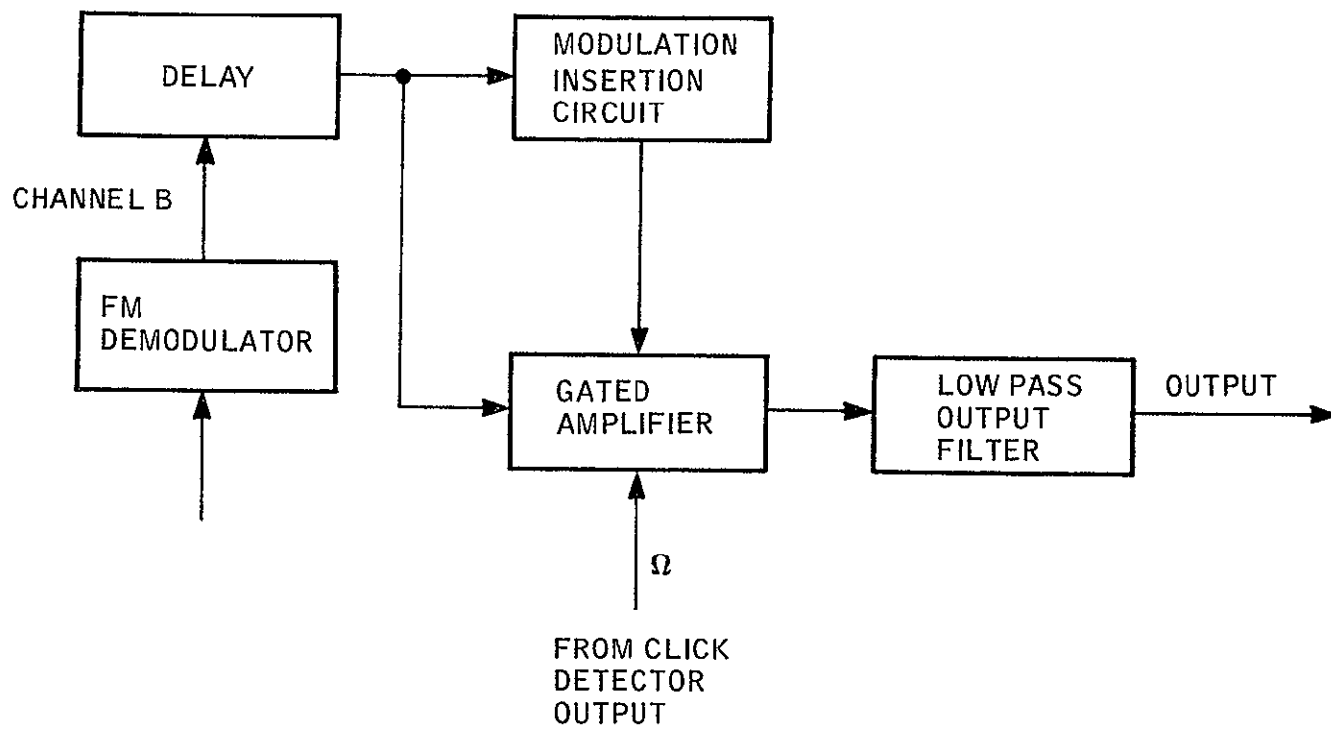


Figure 4-8 Click Eliminator Block Diagram

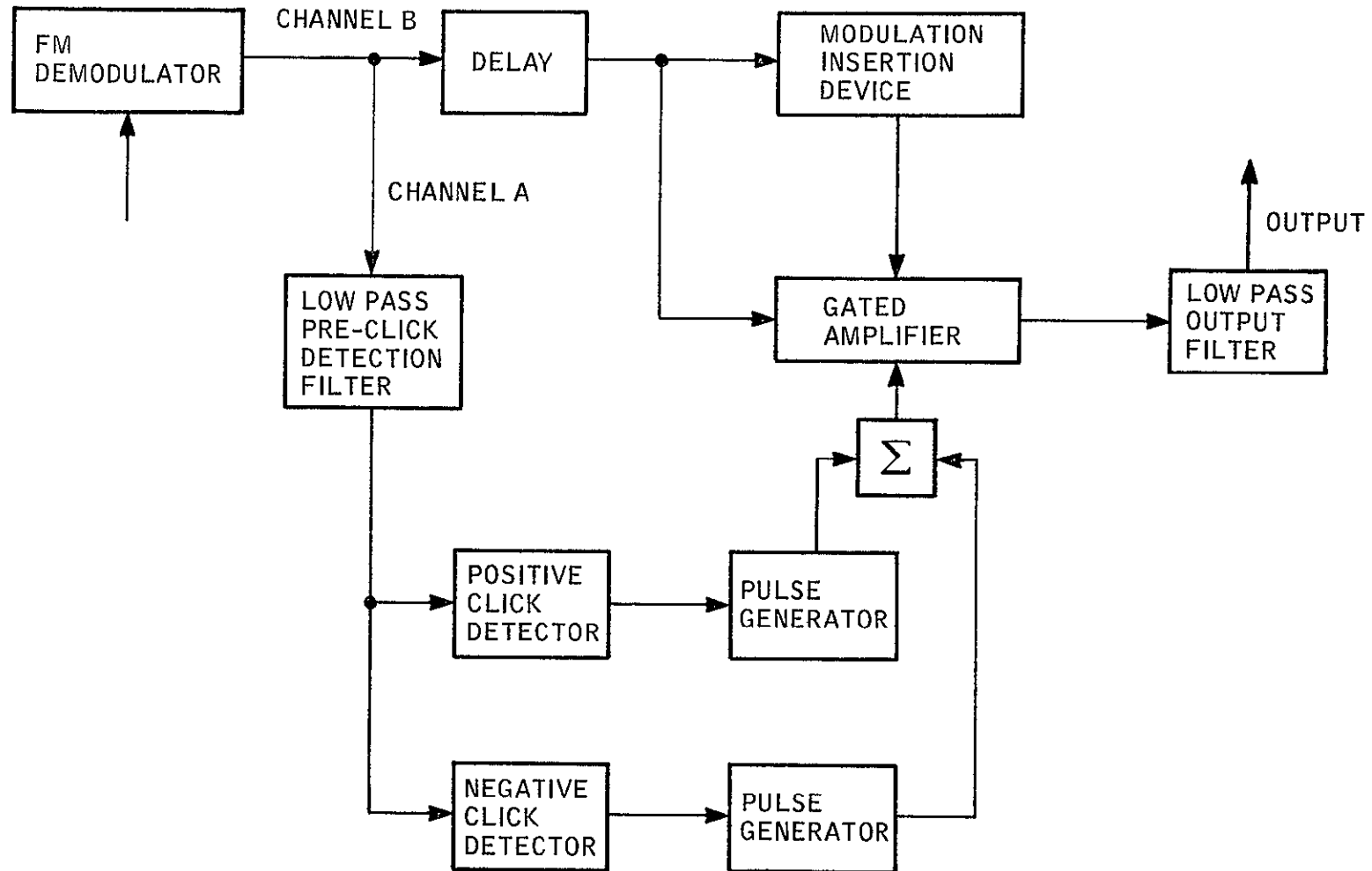


Figure 4-9 Click Detection and Elimination Threshold Extension Device Configuration

4 4 THRESHOLD EXTENSION DEVICE

The following steps summarize the operation of the threshold extension device

- A The output of an FM demodulator, which consists of signal plus noise, is split into two separate channels. The first channel, A, is passed through a pre-click detector filter and is then fed to a series of circuits that detect the presence of high amplitude impulse noise. This is the noise that is a primary factor contributing to the degraded performance of an FM system.
- B The output of the impulse noise detection circuits consists of a series of positive pulses that are fed to a gated amplifier.
- C The input to the gated amplifier is channel B of the demodulator output. Channel B is identical to channel A except that it is time delayed by a preset value.
- D The gating pulses from the noise detection circuits are used to turn off channel B whenever a noise impulse occurs. This creates a "hole" in the channel B output that is smoothed over by additional circuitry which provides an estimate of the modulation during the turnoff time.
- E. The output of the gating amplifier is fed to a low-pass filter that acts to provide additional smoothing to the output modulation during turnoff time.
- F The resulting output consists of signal plus low-level noise with fewer high amplitude impulses to degrade the signal-to-noise ratio.

SECTION 5

EXPERIMENTAL RESULTS

5 1 GENERAL

The performance of the click elimination device has been evaluated in terms of its ability to improve the demodulated output of an Apollo, MSFN, phase-locked loop carrier frequency demodulator. Several tests have been conducted with input signals having parameters representative of the Apollo Block II downlink television and playback voice modes. The signal characteristics of these modes are listed in Table 5-1.

TABLE 5-1

CSM MODES USED FOR THRESHOLD EXTENSION DEVICE TEST

MODE	BASEBAND SERVICE	Δf	f_m	BW_0
CSM FM MODE 1	1 1 PLAYBACK VOICE	100 KHZ	3 KHZ	70 KHZ
CSM FM MODE 2	32 1 PLAYBACK VOICE	100 KHZ	70 KHZ	70 KHZ
CSM FM MODE 4	TV	1.0 MHZ	409 KHZ	500 KHZ

The performance evaluation tests can be outlined as follows:

- A. Signal plus noise waveform analysis
- B. Signal-to-noise ratio tests
 - 1. CSM Modes 1 and 2
 - 2. CSM Mode 4
- C. Voice intelligibility tests
- D. TV picture quality tests

5 2 SIGNAL-PLUS-NOISE WAVEFORM ANALYSIS

A qualitative estimate of the click eliminator performance was obtained by observing the effect of the device on the output noise and signal-plus-noise waveforms as displayed on an oscilloscope. The test configuration is shown in Figure 5-1. The results of this test are shown in Figures 5-2 through 5-13.

The upper trace in each figure represents the unprocessed demodulator output whereas the lower trace shows the click eliminated output.

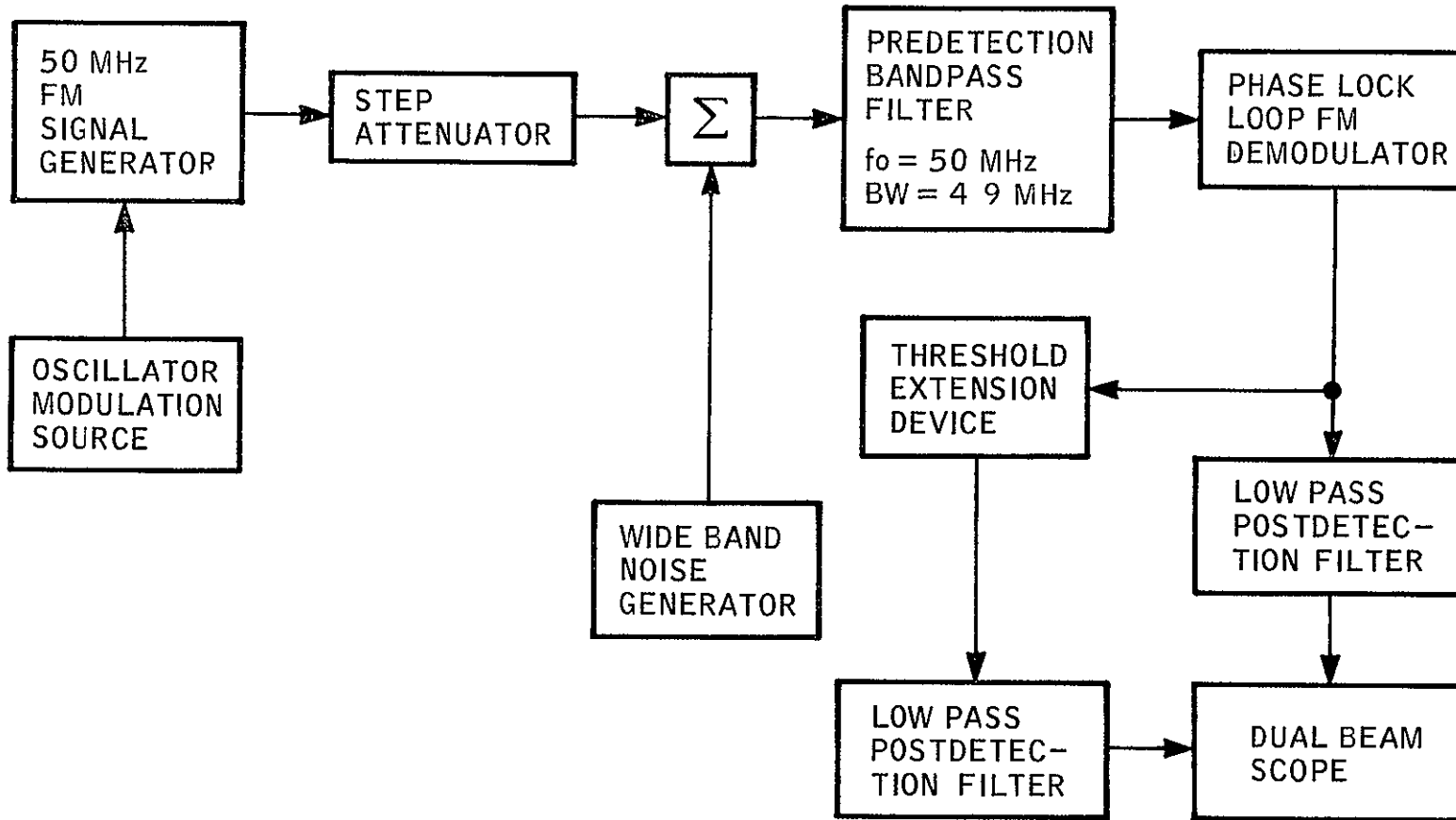
Figures 5-2 and 5-3 show the effectiveness of the click elimination process when the demodulator output consists of noise *without modulation*. The device eliminates 100 percent of the noise spikes for an input signal-to-noise ratio of 3 dB as shown in Figure 5-2. For an input SNR of 1 dB, the elimination process is more than 90 percent efficient. In both cases the postdetection filter was 70 KHz, which corresponds to the CSM Modes 1 and 2 demodulator configuration.

Figures 5-6 through 5-13 show the improvement that is obtained when both sinusoidal signal plus noise are present at the output of the demodulator. The modulation frequencies and deviations (Δf) used for these photographs are compatible with the Apollo CSM FM modes listed in Table 5-1.

Several combinations of modulation frequency and output bandwidth were used to demonstrate the spike noise elimination process for various ratios of click duration to modulation frequency.

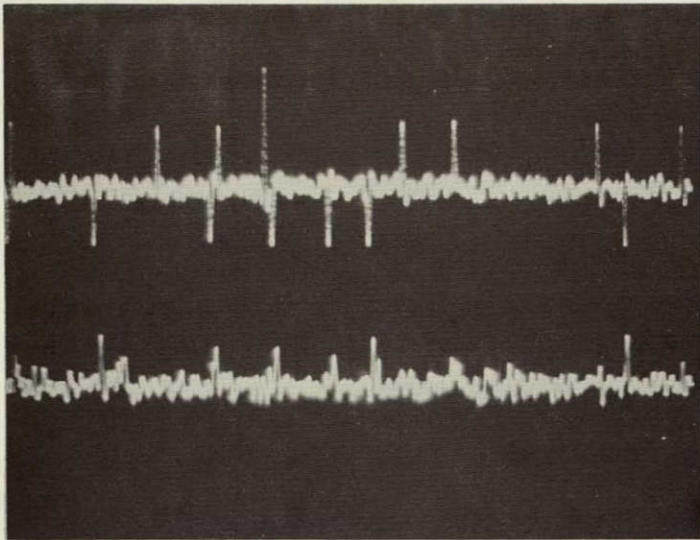
Figures 5-4 and 5-5 illustrate the click elimination process for a modulation frequency of 30 KHz, a peak frequency deviation of 1 MHz, and a postdetection low-pass filter bandwidth of 500 KHz.

For Figures 5-6 and 5-7, the modulation frequency is 1 KHz, the peak frequency deviation is 100 KHz, and the postdetection low-pass filter bandwidth is 70 KHz.



BD10178(A)-4

Figure 5-1 Signal Plus Noise Waveform Analysis Test Configuration



WITHOUT CLICK
ELIMINATION

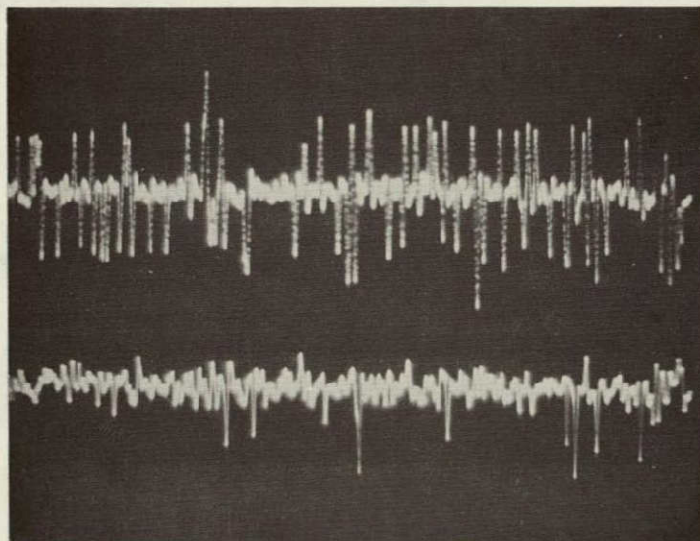
WITH CLICK
ELIMINATION

Figure 5-2 Signal Plus Noise Waveform Analysis

$BW_0 = 70 \text{ KHz}$

$SNR_{IN} = 3\text{dB}$

NO MODULATION



WITHOUT CLICK
ELIMINATION

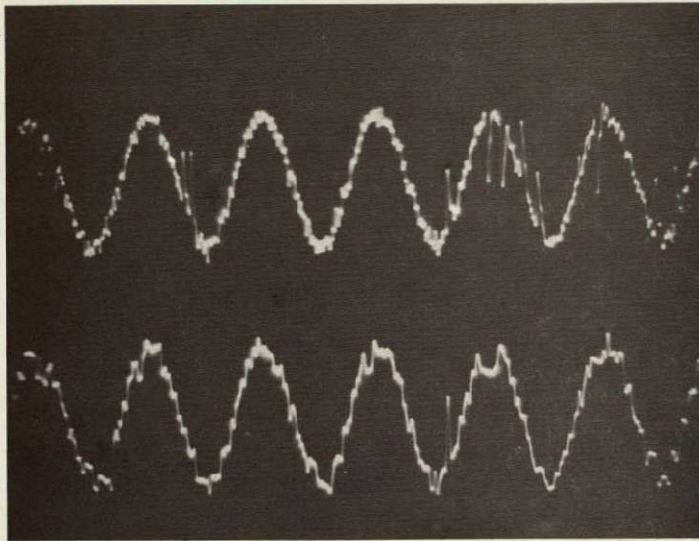
WITH CLICK
ELIMINATION

Figure 5-3 Signal Plus Noise Waveform Analysis

$BW_0 = 70 \text{ KHz}$

$SNR_{IN} = 1\text{dB}$

NO MODULATION

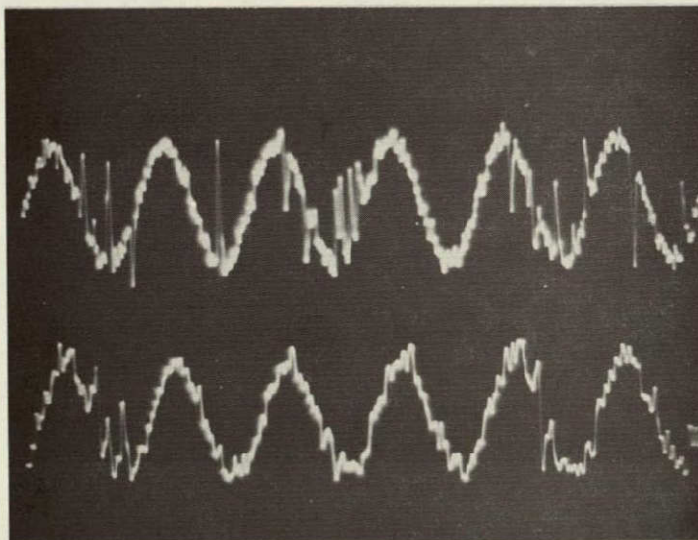


WITHOUT CLICK
ELIMINATION

WITH CLICK
ELIMINATION

Figure 5-4 Signal Plus Noise Waveform Analysis

$f_m = 30 \text{ KHz}$
 $\Delta f = 1 \text{ MHz}$
 $BW_o = 500 \text{ KHz}$
 $SNR_{IN} = 2 \text{ dB}$

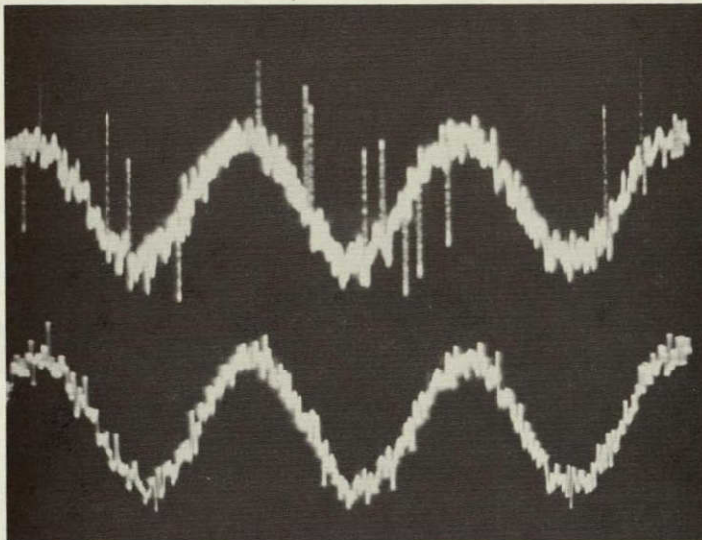


WITHOUT CLICK
ELIMINATION

WITH CLICK
ELIMINATION

Figure 5-5 Signal Plus Noise Waveform Analysis

$f_m = 30 \text{ KHz}$
 $\Delta f = 1 \text{ MHz}$
 $BW_o = 500 \text{ KHz}$
 $SNR_{IN} = 1 \text{ dB}$

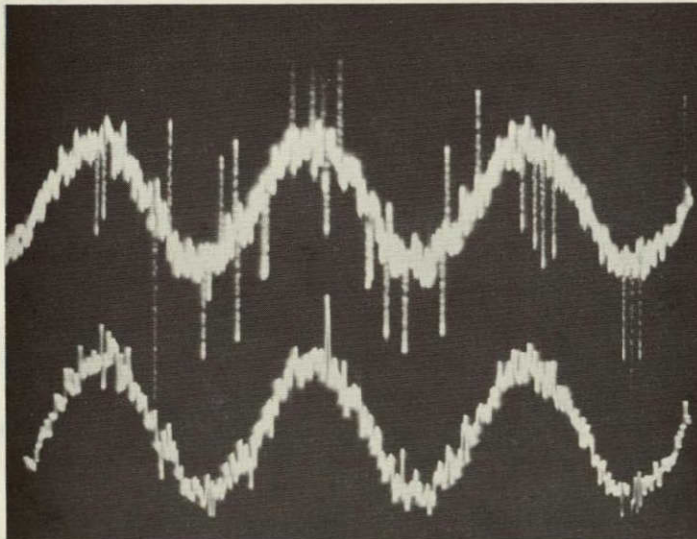


WITHOUT CLICK
ELIMINATION

WITH CLICK
ELIMINATION

Figure 5-6 Signal Plus Noise Waveform Analysis

$f_m = 1 \text{ KHz}$
 $\Delta f = 100 \text{ KHz}$
 $BW_o = 70 \text{ KHz}$
 $SNR_{IN} = 4 \text{ dB}$

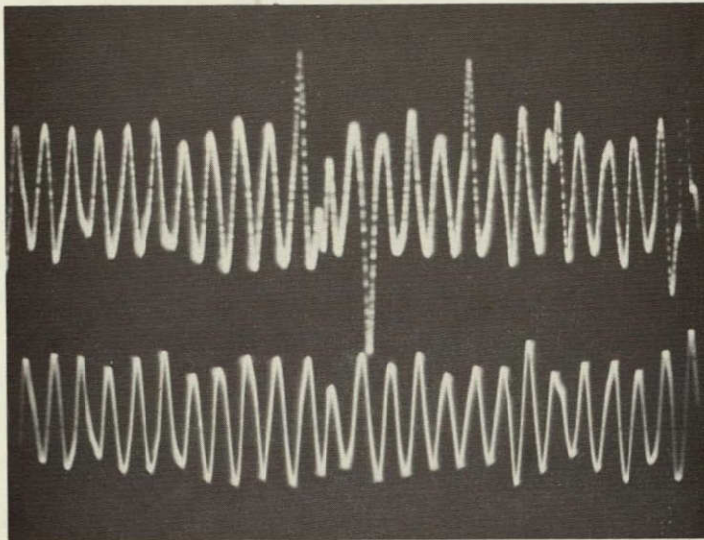


WITHOUT CLICK
ELIMINATION

WITH CLICK
ELIMINATION

Figure 5-7 Signal Plus Noise Waveform Analysis

$f_m = 1 \text{ KHz}$
 $\Delta f = 100 \text{ KHz}$
 $BW_o = 70 \text{ KHz}$
 $SNR_{IN} = 3 \text{ dB}$

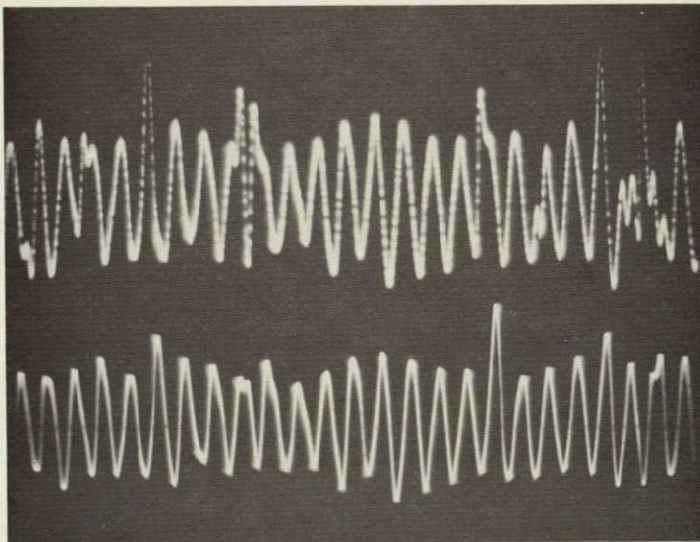


WITHOUT CLICK
ELIMINATION

WITH CLICK
ELIMINATION

Figure 5-8 Signal Plus Noise Waveform Analysis

$f_m = 30 \text{ KHz}$
 $\Delta f = 100 \text{ KHz}$
 $BW_0 = 70 \text{ KHz}$
 $SNR_{IN} = 3 \text{ dB}$

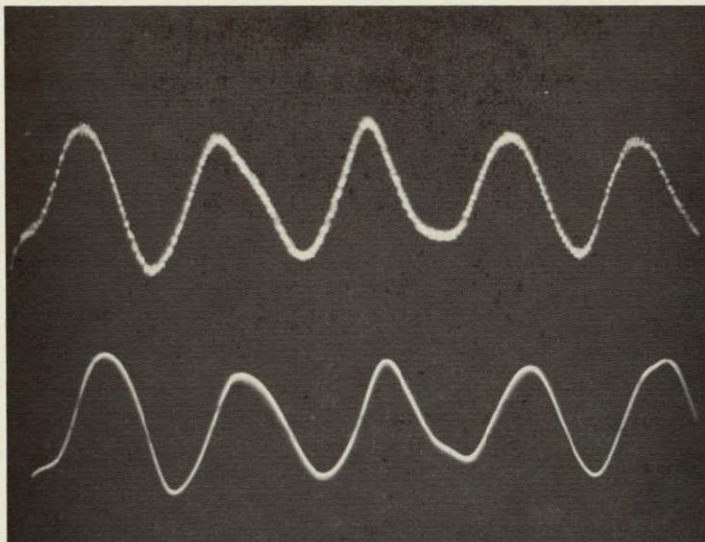


WITHOUT CLICK
ELIMINATION

WITH CLICK
ELIMINATION

Figure 5-9 Signal Plus Noise Waveform Analysis

$f_m = 30 \text{ KHz}$
 $\Delta f = 100 \text{ KHz}$
 $BW_0 = 70 \text{ KHz}$
 $SNR_{IN} = 2 \text{ dB}$

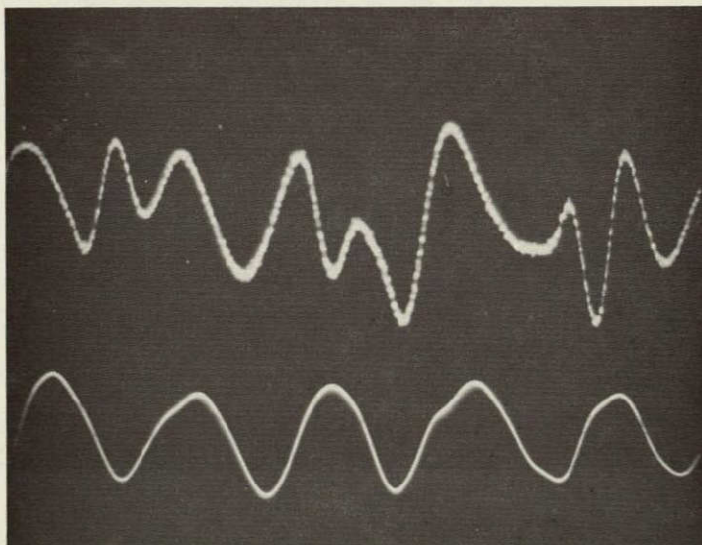


WITHOUT CLICK
ELIMINATION

WITH CLICK
ELIMINATION

Figure 5-10 Signal Plus Noise Waveform Analysis

$f_m = 30 \text{ KHz}$
 $\Delta f = 100 \text{ KHz}$
 $BW_0 = 70 \text{ KHz}$
 $SNR_{IN} = 2 \text{ dB}$

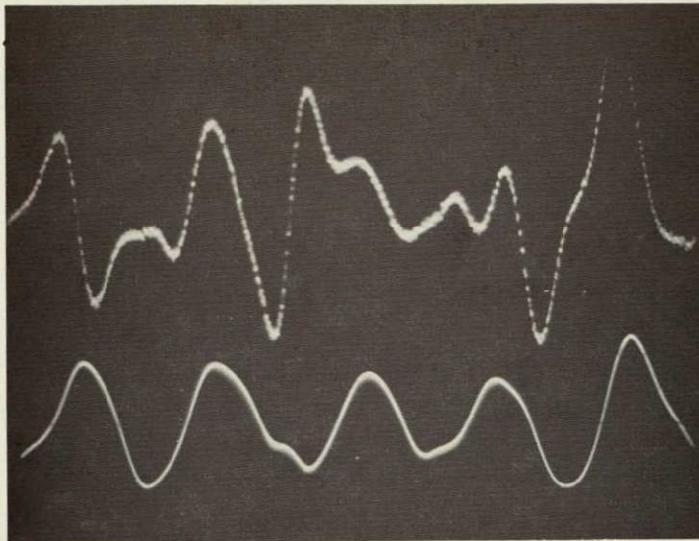


WITHOUT CLICK
ELIMINATION

WITH CLICK
ELIMINATION

Figure 5-11 Signal Plus Noise Waveform Analysis

$f_m = 30 \text{ KHz}$
 $\Delta f = 100 \text{ KHz}$
 $BW_0 = 70 \text{ KHz}$
 $SNR_{IN} = 1 \text{ dB}$

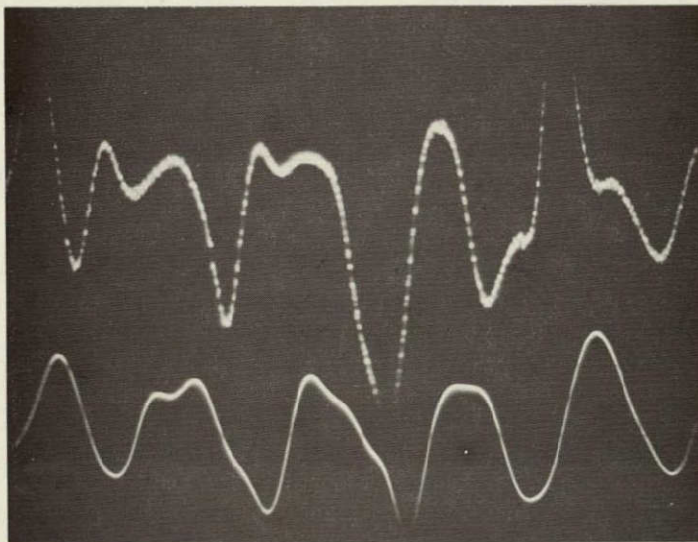


WITHOUT CLICK
ELIMINATION

WITH CLICK
ELIMINATION

Figure 5-12 Signal Plus Noise Waveform Analysis

$f_m = 30 \text{ KHz}$
 $\Delta f = 100 \text{ KHz}$
 $BW_o = 70 \text{ KHz}$
 $SNR_{IN} = 1 \text{ dB}$



WITHOUT CLICK
ELIMINATION

WITH CLICK
ELIMINATION

Figure 5-13 Signal Plus Noise Waveform Analysis

$f_m = 30 \text{ KHz}$
 $\Delta f = 100 \text{ KHz}$
 $BW_o = 70 \text{ KHz}$
 $SNR_{IN} = 1 \text{ dB}$

5.2 SIGNAL-PLUS-NOISE WAVEFORM ANALYSIS (Cont'd)

These figures represent the case where the click duration is small compared to the modulation period. The individual noise spikes do not significantly distort the overall shape of the signal because of their relatively short duration. However, the contribution of the clicks to the output noise power is still considerable because of their relatively high amplitude.

An important observation to be made from Figures 5-4 through 5-7 is that the click eliminator is capable of removing both low-level (those spikes having a peak amplitude less than the maximum modulation amplitude) and high-amplitude spikes from the demodulated waveform. This observation verifies the validity of the criteria for amplitude detection of click noise in the unfiltered demodulator output.

In Figures 5-8 through 5-13, the modulation frequency is 30 KHz; the peak frequency deviation is 100 KHz; and the postdetection low-pass filter bandwidth is 70 KHz. These figures represent the case where the click duration is approximately equal to half the modulation period. This means that a single noise spike will cause considerable distortion to the shape of the demodulated signal waveform.

Figures 5-8 through 5-13 illustrate the ability of the click eliminator to provide a modulation estimate as a substitute for the distortion caused by the occurrence of a noise spike on the output waveform. It should be noted that, in most cases, the noise spikes occur when the modulation amplitude is at a maximum.

5.3 SIGNAL-TO-NOISE RATIO TESTS

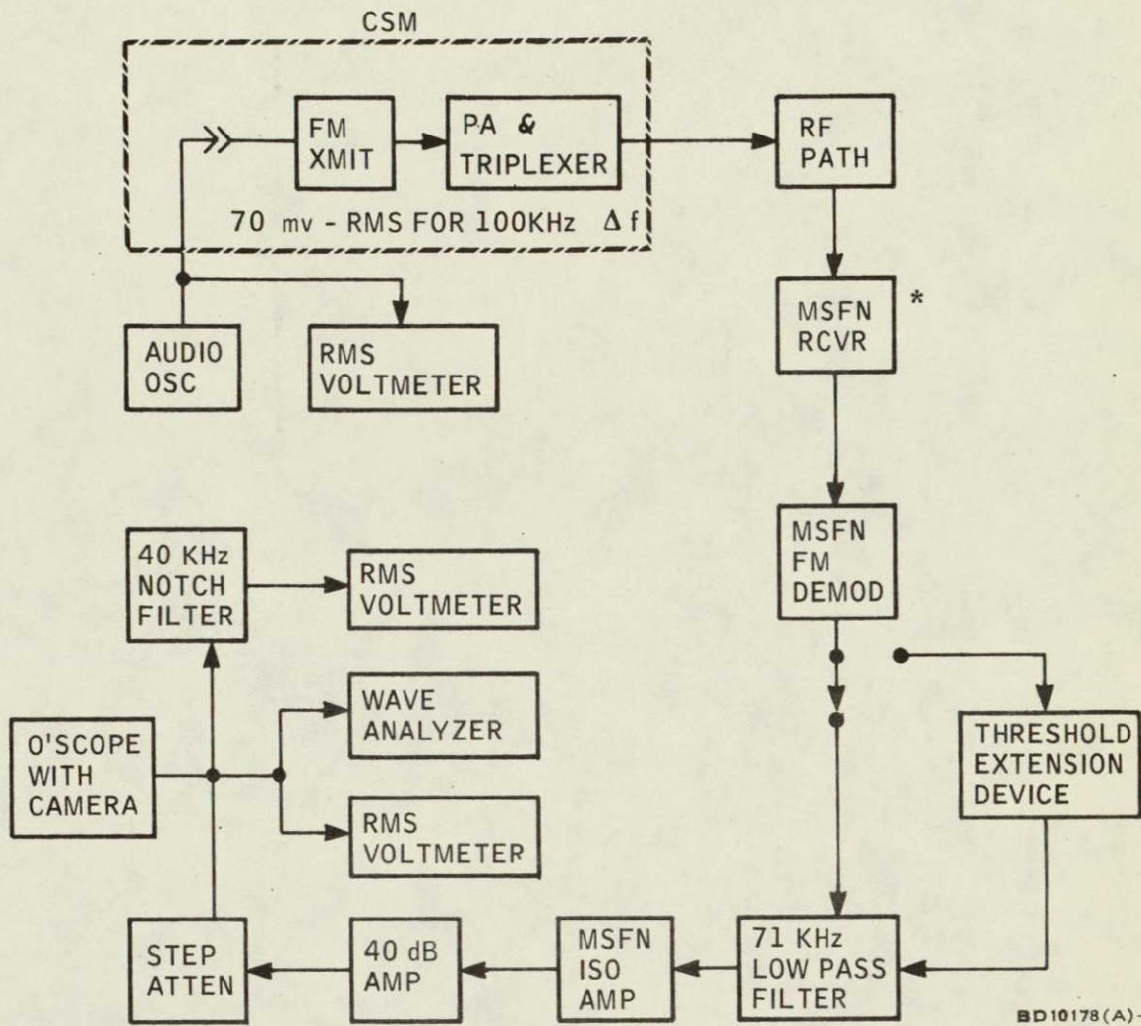
5.3.1 CSM FM Modes 1 and 2

A quantitative evaluation of the click eliminator's ability to improve the performance of an FM channel can be obtained by determining the threshold extension that results from the suppression of spike noise. The threshold extension can be determined by measuring the output signal-to-noise ratio of an FM demodulator before and after the click elimination process.

These tests were performed with a simulated Apollo Block II CSM-to-MSFN playback voice channel in the Electronics Systems Compatibility Laboratory (ESCL) of ISD/MS. The ESCL contains an Apollo MSFN ground station receiver that was used in conjunction with a simulated RF path and CSM transponder as shown in Figure 5-14. The click elimination device was inserted between the output of the carrier frequency demodulator and the 71-KHz low-pass postdetection filter.

The output signal-to-noise ratio was measured with and without the click eliminator in the system for a wide range of received signal levels. Figure 5-15 represents the measured data for the 1:1 playback voice mode test. The threshold point is approximately -90.6 dBm for the unprocessed channel and -92.7 dBm for the click eliminated channel. The difference between these two values of total received RF power represents the effective threshold extension obtained with the click elimination device. From Figure 5-15 it can be determined that a 2-dB extension of threshold was obtained for the Apollo CSM Mode 1. However, the improvement in output SNR is significantly greater than indicated by the 2-dB threshold extension. A maximum improvement of 8 dB to 10 dB is obtained for certain values of total received power that are below the threshold points found in Figure 5-15. The significance of this SNR improvement will be shown in the results of the word intelligibility tests.

Figure 5-16 represents the measured data for the 32:1 playback voice mode test. The threshold point is approximately -89.0 dBm for the unprocessed channel and -90.4 for the click eliminated channel. A threshold extension of approximately 1.5 dB was achieved for this mode, while the maximum output SNR improvement was 10 dB. A 1-KHz tone was used as modulation for the CSM Mode 2 tests.



BD10178(A)-8

*NOTE: The test configuration MSFN receiver does not include a paramp and, therefore, has a noise figure of approximately 10 dB.

Figure 5-14 Test Configuration for CSM Modes 1 and 2 Signal-to-Noise Ratio Tests With and Without Threshold Extension Device

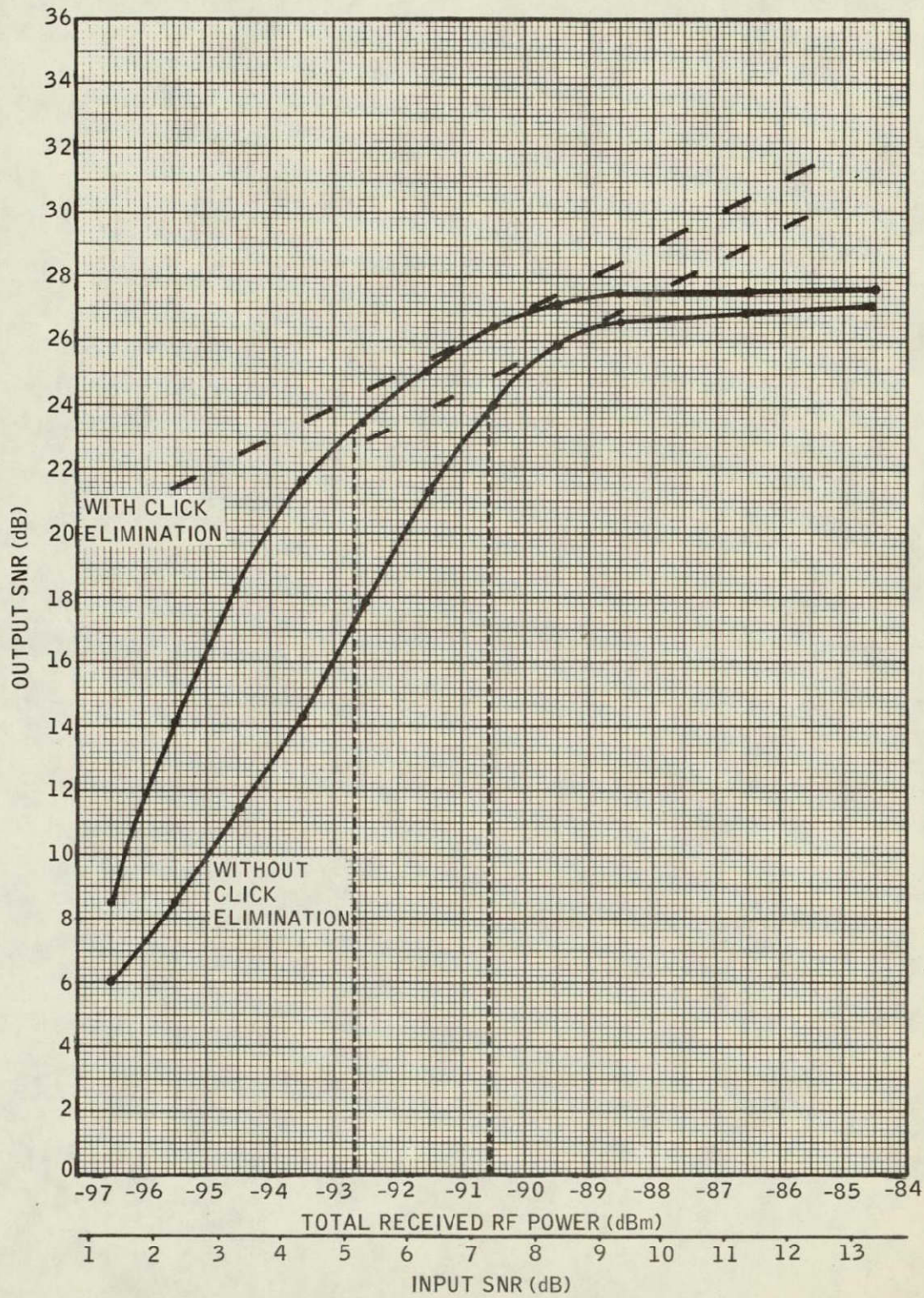


Figure 5-15 Output SNR vs Input SNR for 1:1 CSM Playback Voice Mode

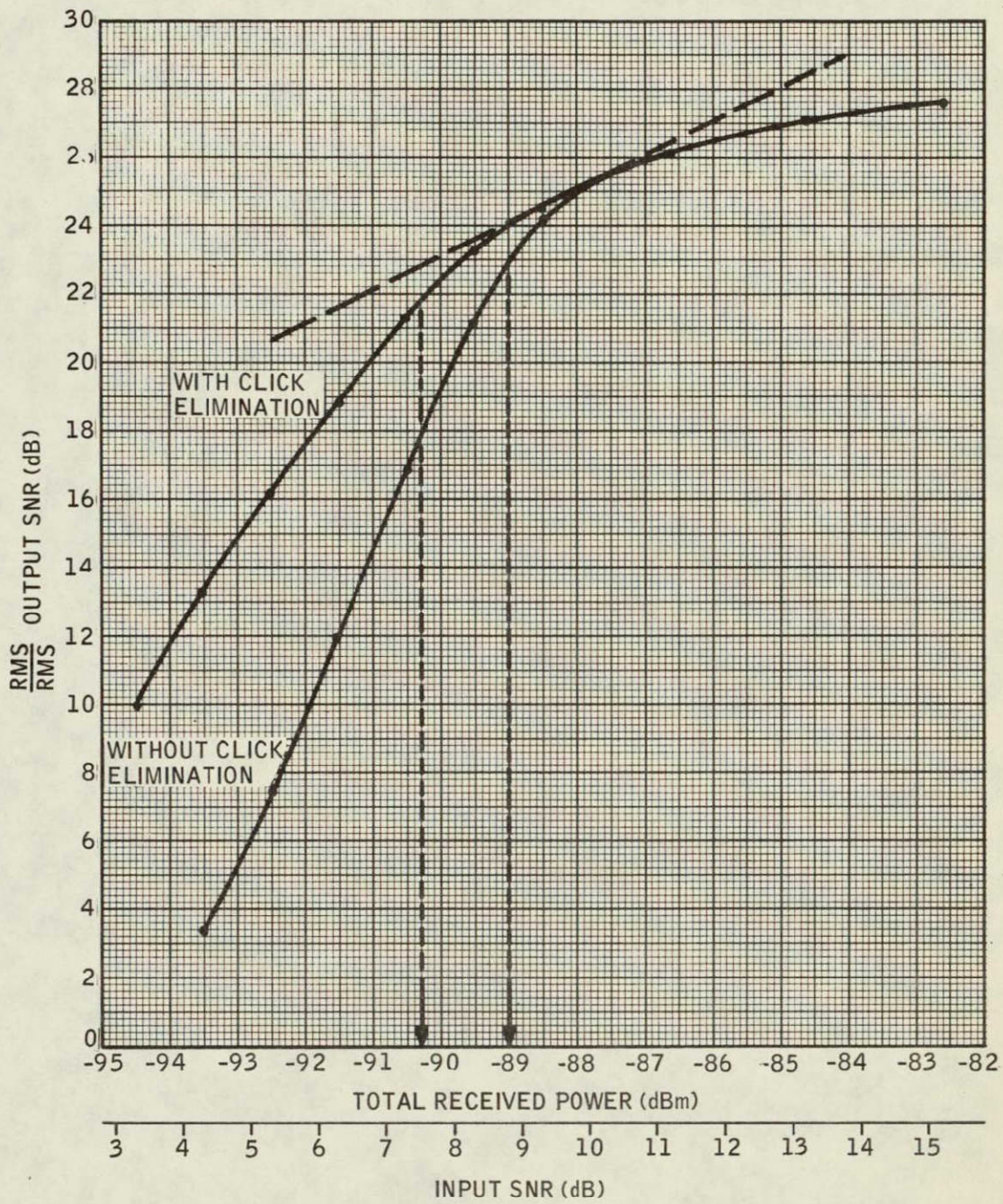


Figure 5-16 Output SNR vs Input SNR for 32:1 CSM Playback Voice Mode

GC10177(A)-5

5.3.1 CSM FM Modes 1 and 2 (Cont'd)

It should be noted that in both Figure 5-15 and 5-16 the measured data does not agree with the theoretical one-to-one output vs input SNR relationship expected for large values of input SNR. Instead, the measured curves flatten such that the output SNR remains almost constant for values of input SNR greater than 12 dB. This limiting effect is due to the presence of three scientific subcarriers which are part of CSM FM Modes 1 and 2. The subcarrier frequencies are close enough to the playback voice bandpass to limit the output SNR at large values of input SNR.

Straight lines have been drawn tangent to the measured curve with a slope of 1 for the purpose of determining the threshold point for Figure 5-15 and 5-16. The threshold point was then determined graphically according to the procedure discussed in Section 3.1.

A plot of the output SNR improvement versus input SNR is shown in Figure 5-17. The maximum improvement occurs for values of input SNR between 3 dB and 5 dB for both modes. The click eliminator improvement increases linearly as the input SNR decreases from approximately 9 dB to 5 dB. For values of input SNR below 3 dB, the improvement drops off rapidly due to saturation of the click noise detection circuits. It is possible that this saturation effect could actually degrade the output performance of the demodulator. This would occur when the number of clicks per second is such that the output of the click eliminator is turned off most of the time.

5.3.2 CSM FM Mode 4

The system configuration for the CSM television mode test is shown in Figure 5-18. A 300-KHz tone was used to modulate the 50-MHz FM test set. A threshold improvement of 1.5 dB was obtained as shown in Figure 5-19. The maximum improvement in output SNR was found to be approximately 8 dB. It should be noted that the shape of the plot representing the performance of the demodulator with click elimination is considerably more linear than the curve representing the performance of the same demodulator without click elimination.

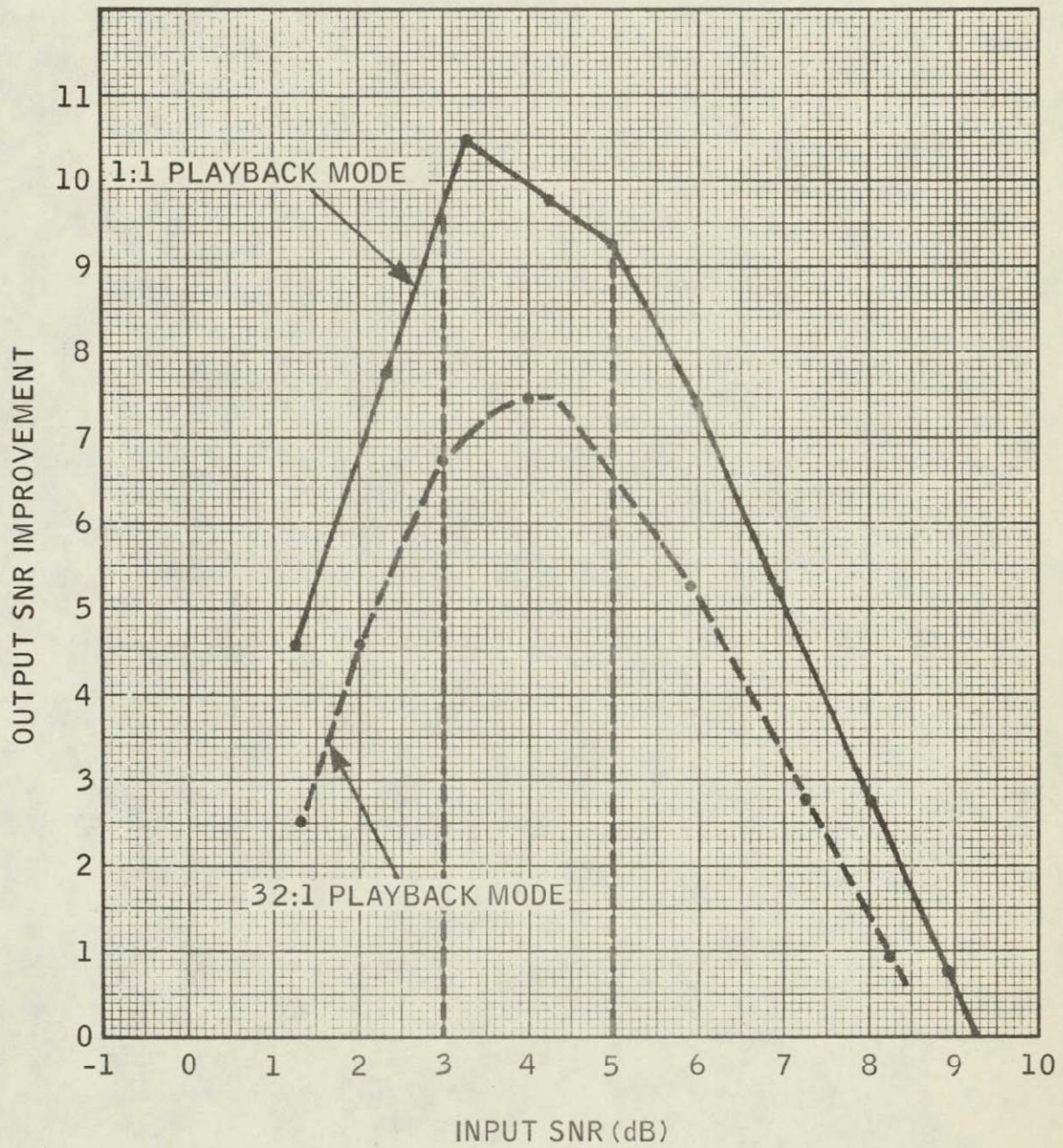


Figure 5-17 Output SNR Improvement vs Input SNR for 1:1 and 32:1 CSM Playback Voice

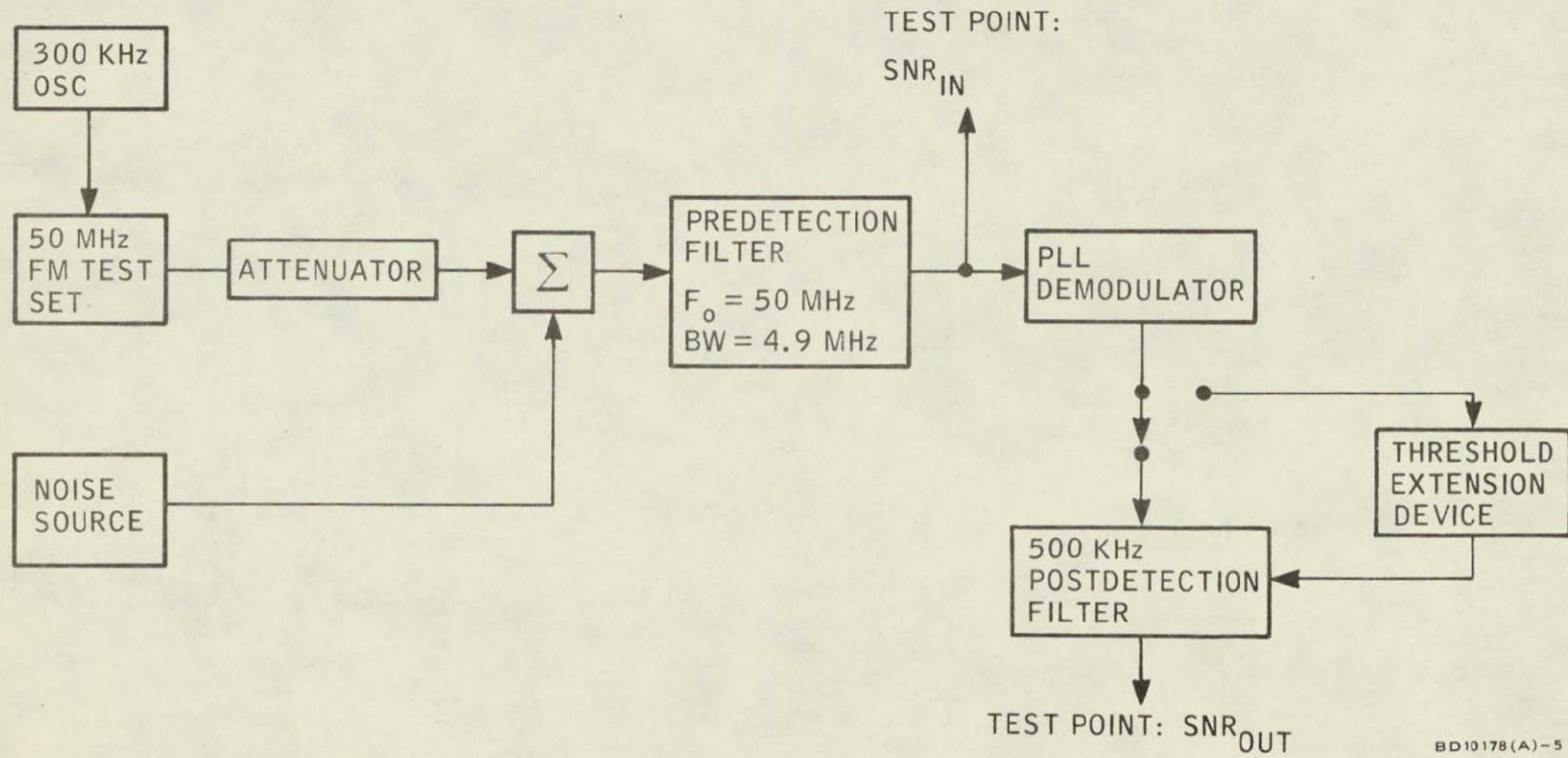


Figure 5-18 Configuration for CSM Mode 4 SNR Tests

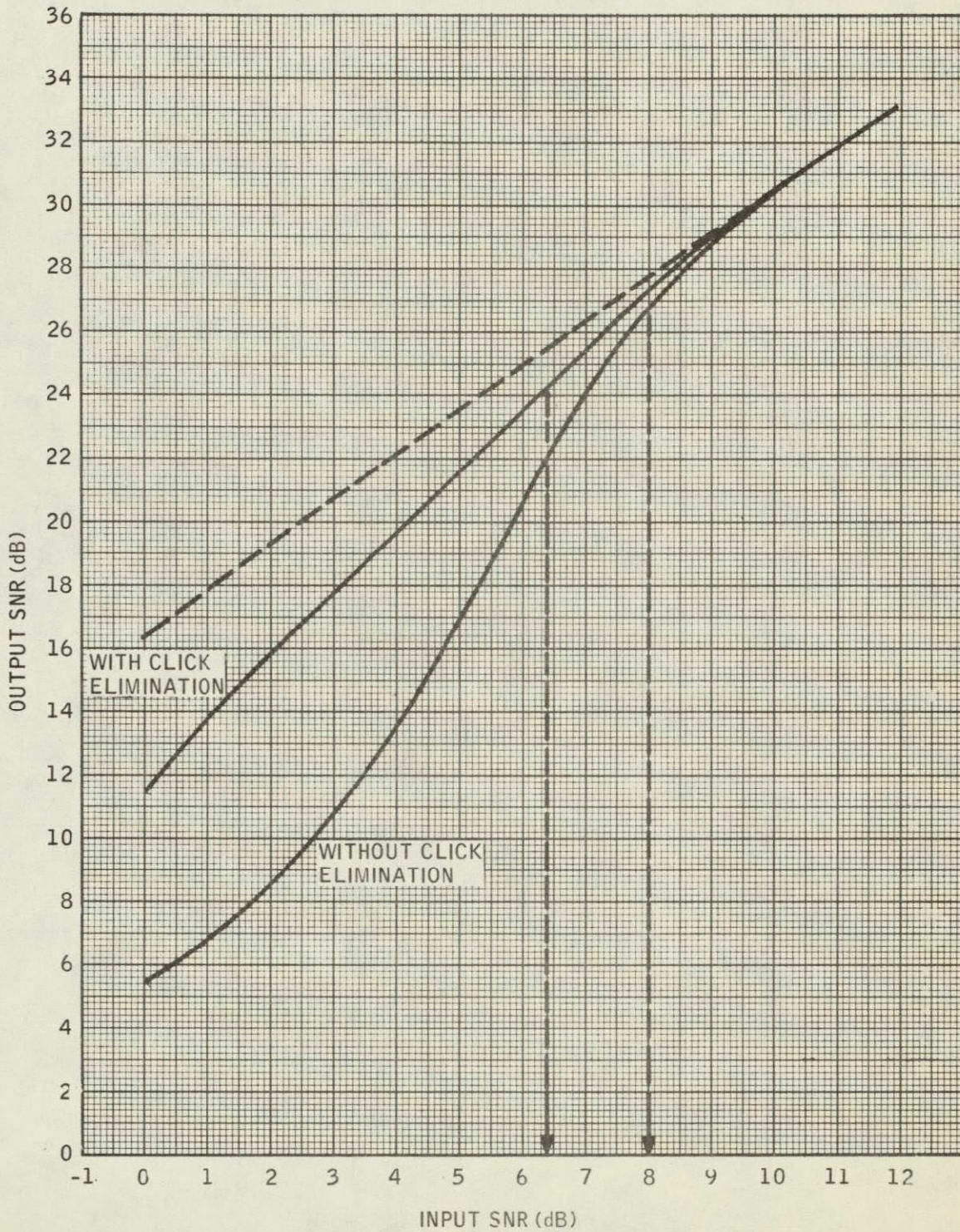


Figure 5-19 Output SNR vs Input SNR for CSM FM Mode 4

GC10177(A)-4

5.3.2 CSM FM Mode 4 (Cont'd)

The implication of this observation is that the rapid deterioration of the output signal which is normally associated with the operation of an FM demodulator below threshold can be significantly reduced by the application of click noise elimination techniques. Therefore, an input SNR of 3 dB would probably result in a "useless" output signal for a demodulator without click elimination whereas the corresponding output signal from the demodulator using click elimination might be useful.

A plot of output SNR improvement versus input SNR for CSM Mode 4 is shown in Figure 5-20. The maximum improvement is obtained for values of input SNR between 1 and 3 dB.

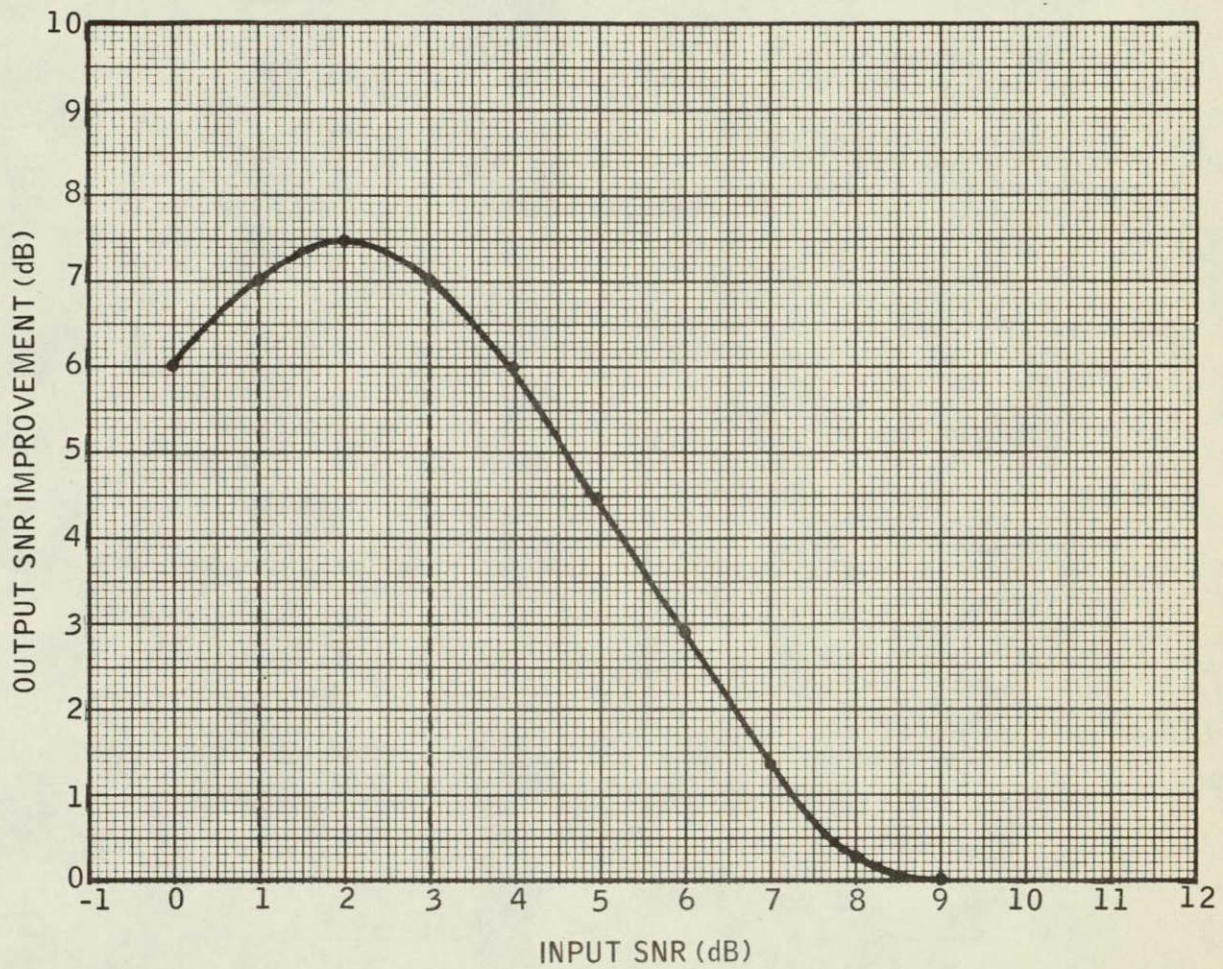


Figure 5-20 Output SNR Improvement vs Input SNR
for CSM FM Mode 4 With Click Elimination

GC10177(A)-8

5.4 WORD INTELLIGIBILITY TESTS

Experimental results from the signal-to-noise ratio tests indicate that a threshold improvement of 1.5 dB to 2 dB was obtained for CSM Modes 1 and 2, while the maximum output SNR improvement for the modes was 8 dB to 10 dB.

A more realistic evaluation of the click elimination performance, however, can be obtained by determining the improvement in output word intelligibility. Several tests were conducted, using the configuration shown in Figure 5-21, for the 1:1 playback voice mode. The pre-recorded voice tapes used to modulate the CSM FM transmitter were composed of 150 words separated into three groups. Each group of 50 words was spoken by a different person. A different word list tape was used for each test run representing a specific value of total received power, and the demodulated information was recorded for later evaluation of the output word intelligibility.

The results of the word intelligibility tests are shown in Figure 5-22. The maximum improvement in word intelligibility was approximately 20 percent for an input SNR of 4.3 dB. Referring to Figure 5-17, this value of input SNR lies within the region of maximum improvement (between 3 dB and 5 dB input SNR) for this particular mode.

The results of the word intelligibility tests for the 32:1 playback mode are shown in Figure 5-24. The improvement obtained for this mode is considerably less than that obtained for the 1:1 playback mode. A maximum improvement of only 4 percent in word intelligibility occurred for an input SNR of 6.3 dB. The difference between the improvement observed for these two modes is related to the distortion inherent in the spacecraft playback system. It should be noted that even at relatively high values of input SNR the intelligibility is limited to 81 percent for the 32:1 playback mode, whereas 91 percent intelligibility is obtained for the 1:1 playback mode for the same input SNR. The 32:1 playback voice tests were performed with the test configuration shown in Figure 5-23.

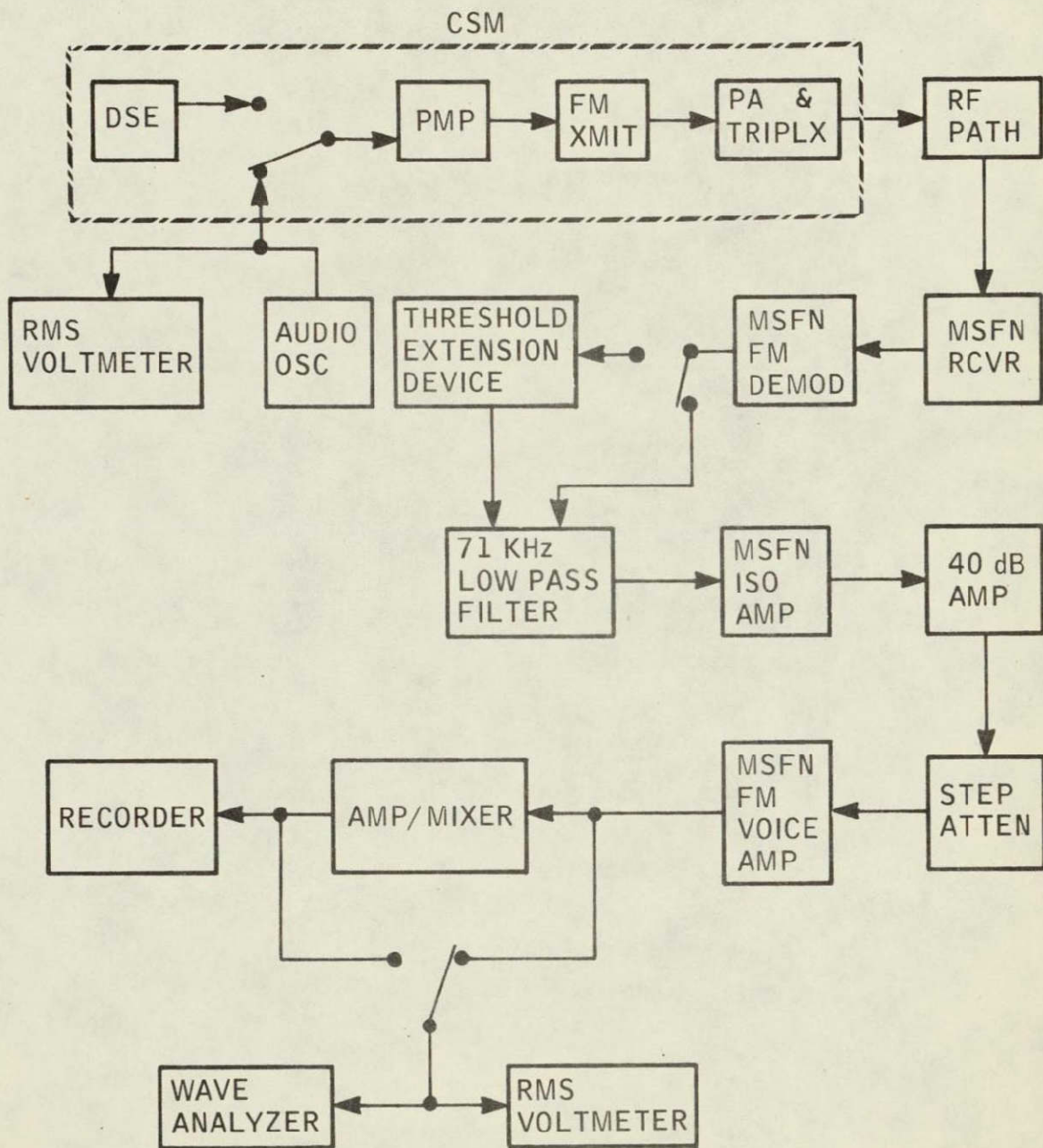


Figure 5-21 Configuration for CSM FM Mode 1 Word Intelligibility Test With and Without Threshold Extension Device

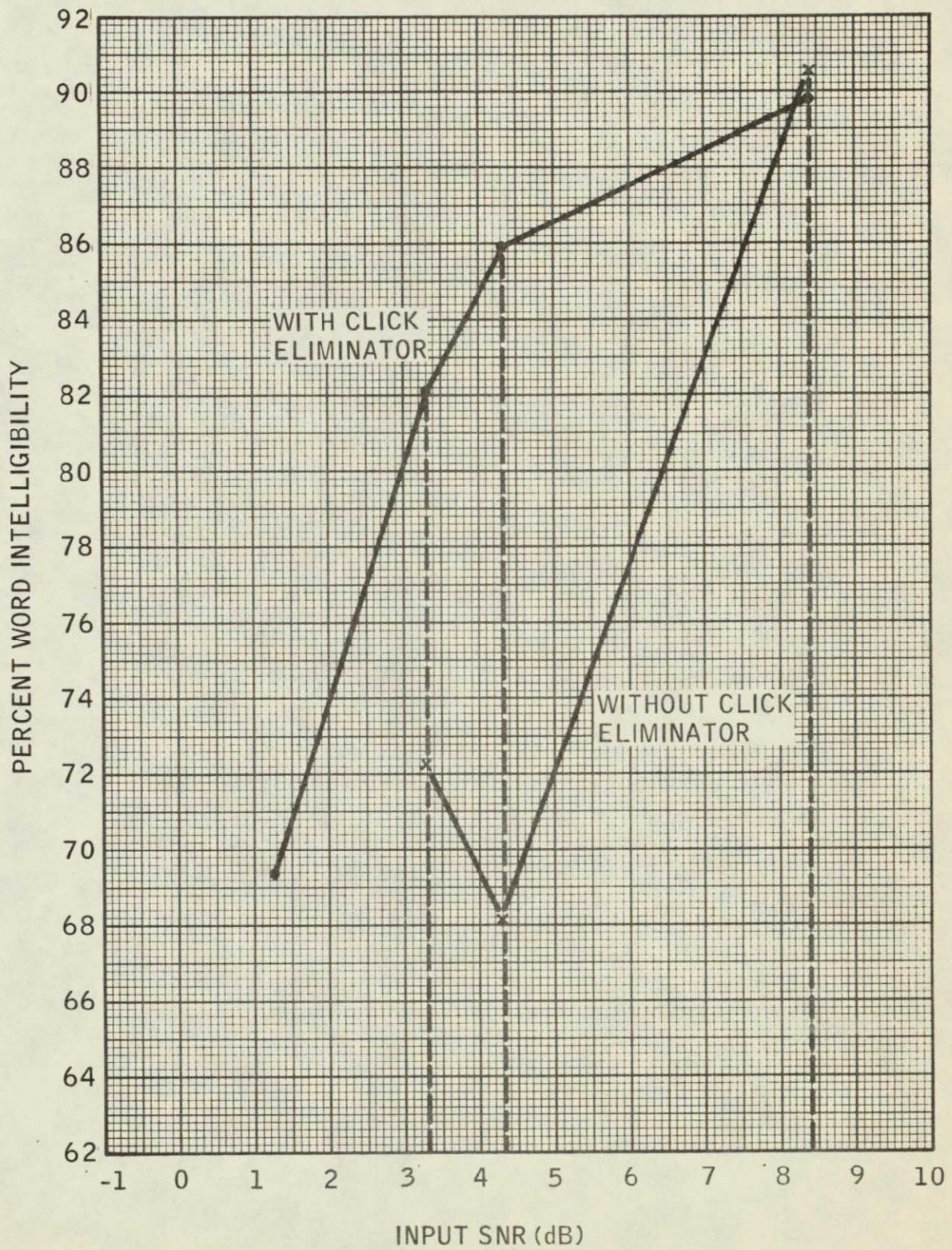


Figure 5-22 Percent Word Intelligibility vs Input SNR for 1:1 CSM Playback Voice Mode

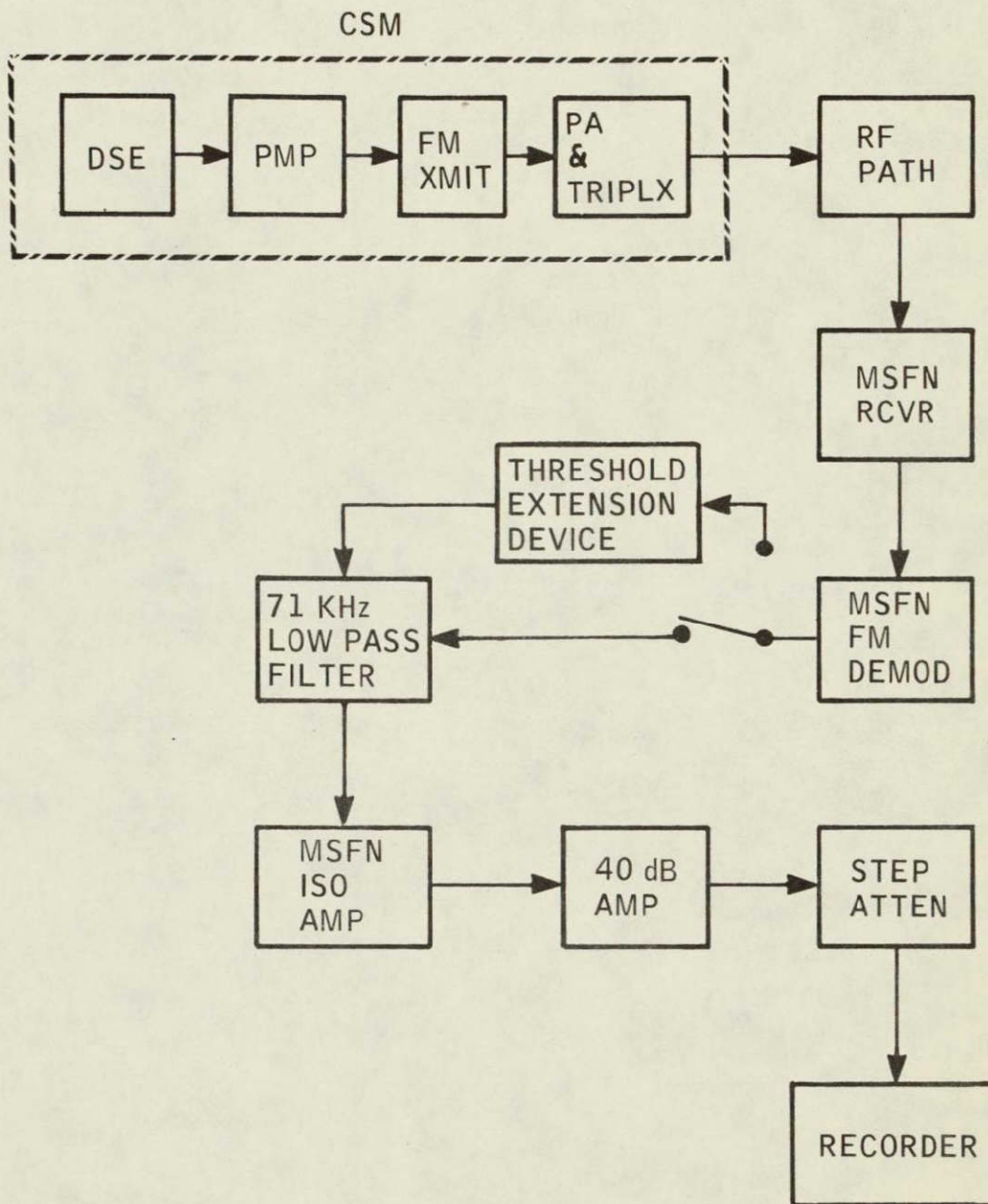


Figure 5-23 Configuration for CSM FM Mode 2 Word Intelligibility Tests With and Without Threshold Extension Device

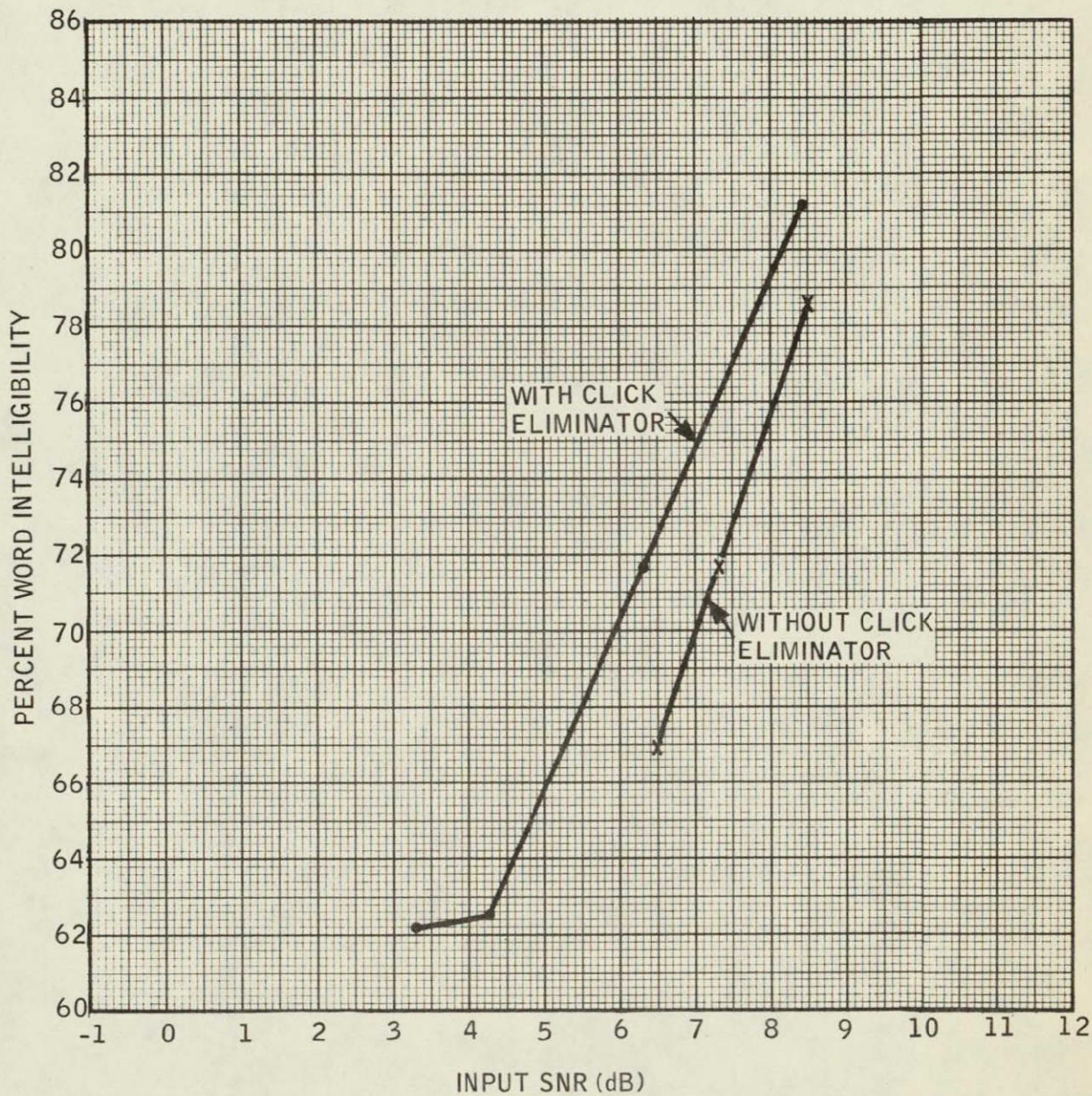


Figure 5-24 Percent Word Intelligibility vs Input SNR for CSM 32:1 Playback Voice Mode

GC10177(A)-7

5.5 TELEVISION PICTURE QUALITY ANALYSIS

The test configuration shown in Figure 5-25 was used to obtain a series of photographs representing the demodulated video signal output of an Apollo type FM demodulator. The demodulated signal was displayed on the CRT of a slow scan monitor operating in the CSM-LM Block II, 10 frame-per-second mode. The photographs were taken with equal exposure times of 1/10 second and with a constant camera aperture. Therefore, each picture represents one complete frame of information.

A grey scale signal was used to modulate the FM test set with a peak frequency deviation of 1.0 MHz. Figure 5-26 shows the demodulated signal displayed on the slow scan monitor for a 20-dB input SNR. This picture is used primarily as a calibration reference to which the following data will be compared.

Figure 5-27 shows the demodulated output for a 10-dB input SNR. The presence of Gaussian noise results in a "fuzzy" picture as compared with Figure 5-26. The absence of click noise in these pictures indicates that the demodulator is operating above threshold.

The presence of click noise, which appears as white or black spots on the photograph, is first noticed in Figure 5-28 for an input SNR of 8 dB. Although only two or three clicks can be found in this figure, one of them has resulted in a momentary loss of line synchronization as indicated by the torn segment of the vertical white bar. The synchronization circuitry in the MSFN slow scan monitor is particularly sensitive to the presence of click noise. Figure 5-29 shows the demodulated output for an 8 dB input SNR with the click eliminator in the system. Notice that the click noise has been eliminated and that the line synchronization has been preserved.

As the input SNR is decreased to 7 dB, the demodulator approaches threshold, and the number of clicks, as well as synchronization perturbations, increases accordingly.

Figures 5-30 and 5-31 show the demodulated signal before and after the click elimination process for an input SNR of 7 dB. Figures 5-32 and 5-33 provide similar results for an input SNR of 6 dB (the click eliminator has been able to dispose of almost every click for values of input SNR down to 6 dB. For SNR's below

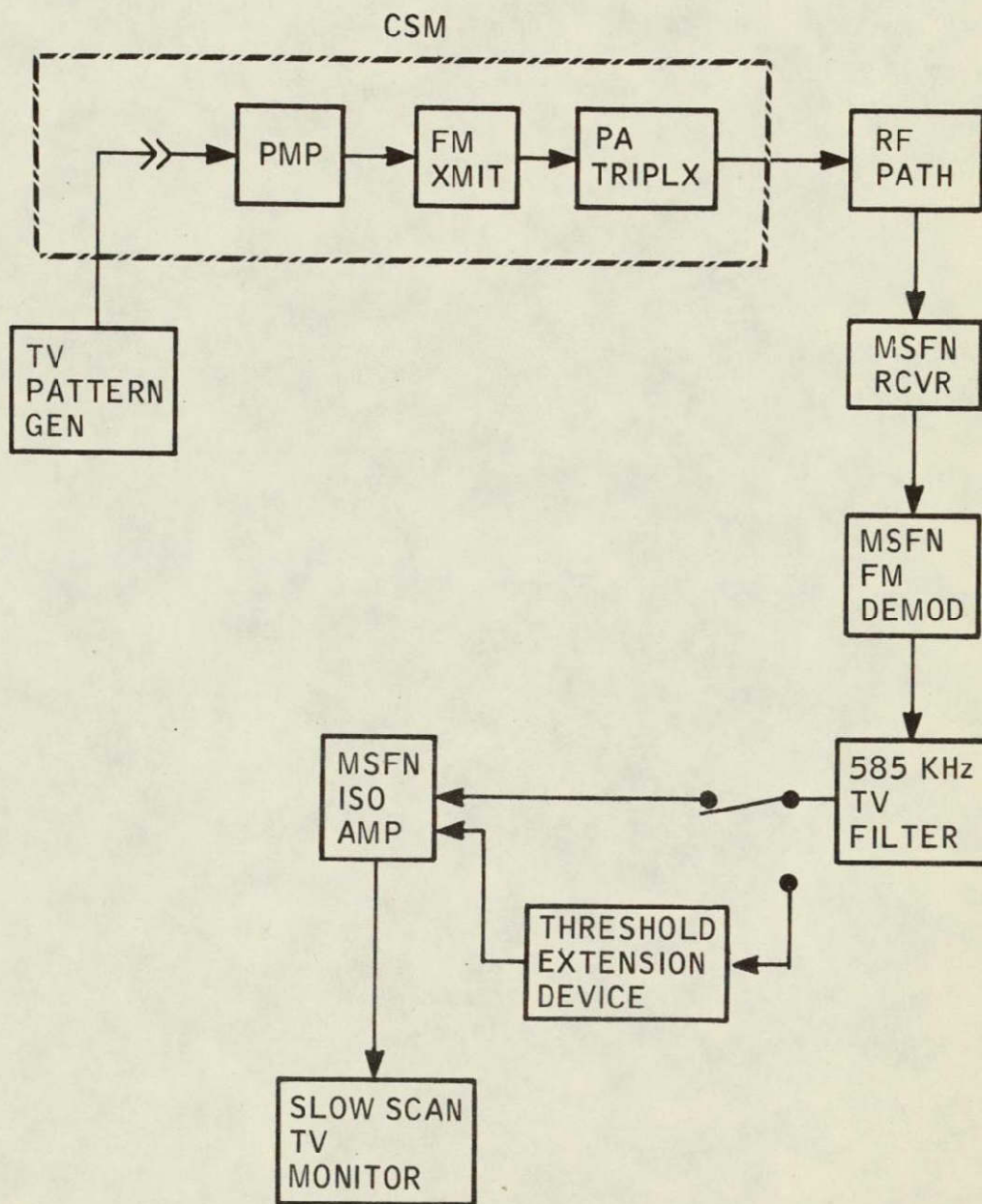
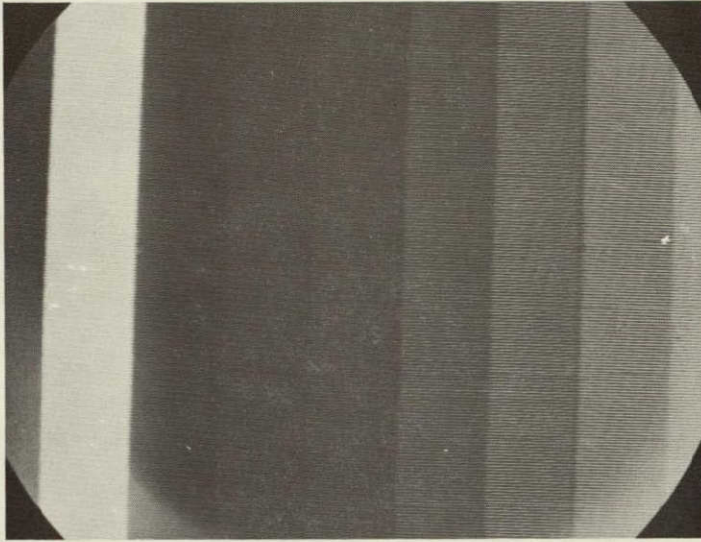


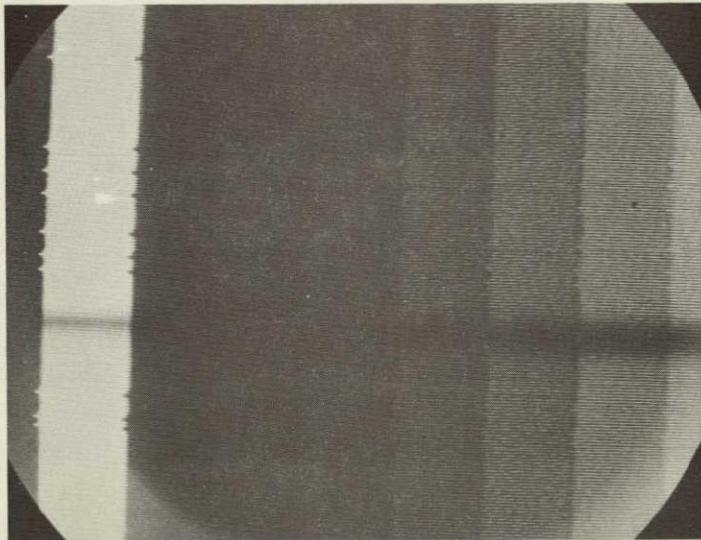
Figure 5-25 Configuration for CSM Mode 4
Television Picture Quality Tests



$\Delta f = 1.0 \text{ MHz}$
 $BW_{IF} = 4.9 \text{ MHz}$
 $BW_o = 500 \text{ KHz}$

Figure 5-26 CSM Mode 4: TV Picture Quality Tests

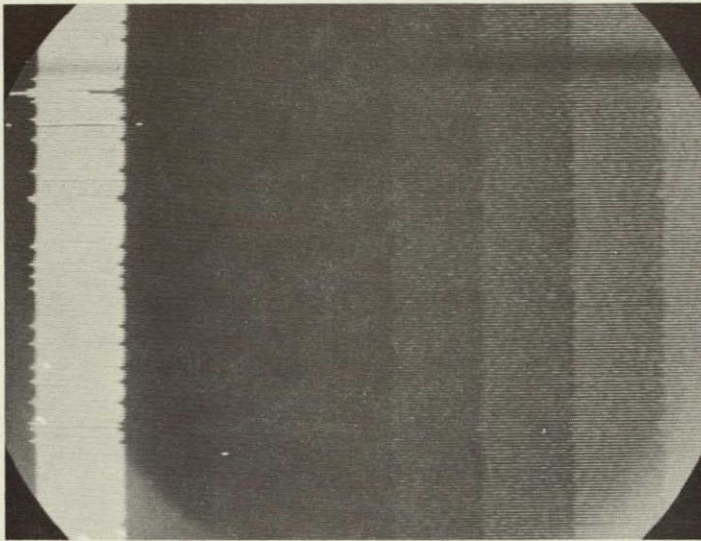
$SNR_{IN} = 20 \text{ dB}$ REFERENCE PICTURE



$\Delta f = 1.0 \text{ MHz}$
 $BW_{IF} = 4.9 \text{ MHz}$
 $BW_o = 500 \text{ KHz}$

Figure 5-27 CSM Mode 4: TV Picture Quality Tests

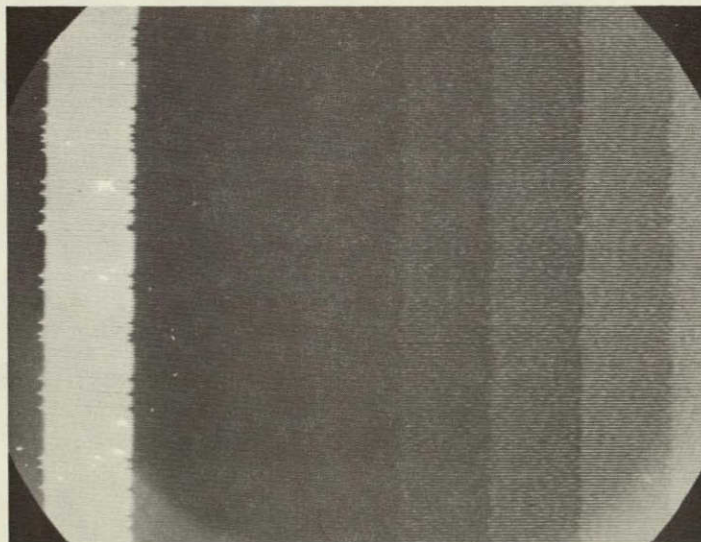
$SNR_{IN} = 10 \text{ dB}$ WITHOUT CLICK ELIMINATION



$\Delta f = 1.0 \text{ MHz}$
 $BW_{IF} = 4.9 \text{ MHz}$
 $BW_0 = 500 \text{ KHz}$

Figure 5-28 CSM Mode 4: TV Picture Quality Tests

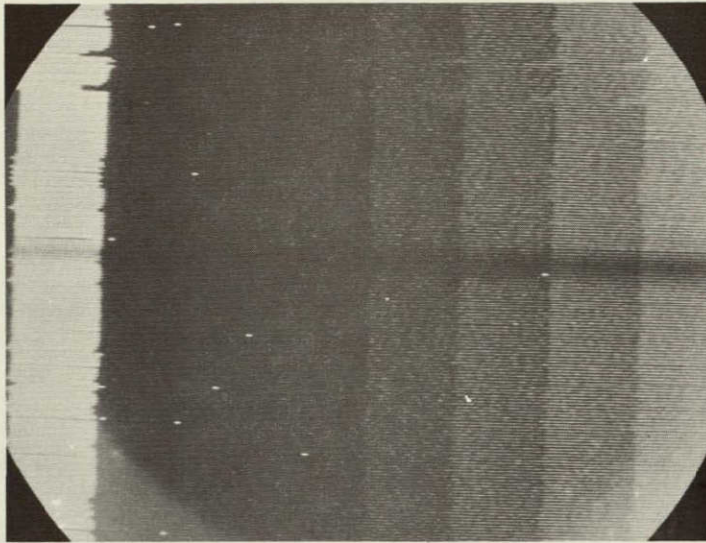
$SNR_{IN} = 8 \text{ dB}$ WITHOUT CLICK ELIMINATION



$\Delta f = 1.0 \text{ MHz}$
 $BW_{IF} = 4.9 \text{ MHz}$
 $BW_0 = 500 \text{ KHz}$

Figure 5-29 CSM Mode 4: TV Picture Quality Tests

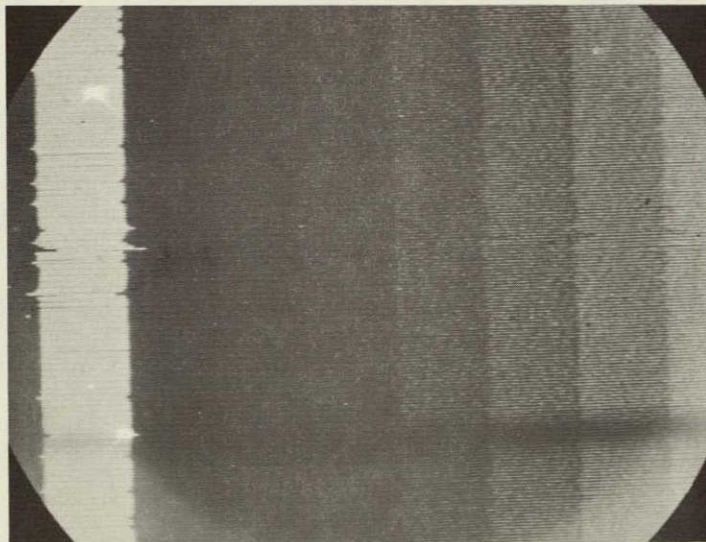
$SNR_{IN} = 8 \text{ dB}$ WITH CLICK ELIMINATION



$\Delta f = 1.0 \text{ MHz}$
 $BW_{IF} = 4.9 \text{ MHz}$
 $BW_o = 500 \text{ KHz}$

Figure 5-30 CSM Mode 4: TV Picture Quality Tests

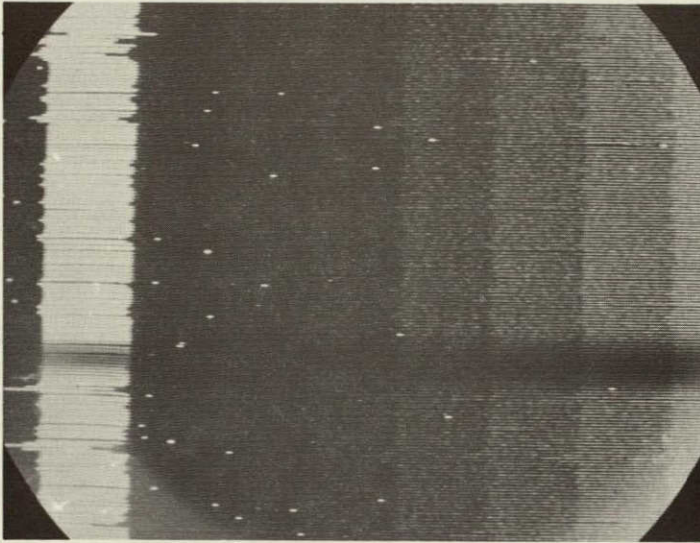
$SNR_{IN} = 7 \text{ dB}$ WITHOUT CLICK ELIMINATION



$\Delta f = 1.0 \text{ MHz}$
 $BW_{IF} = 4.9 \text{ MHz}$
 $BW_o = 500 \text{ KHz}$

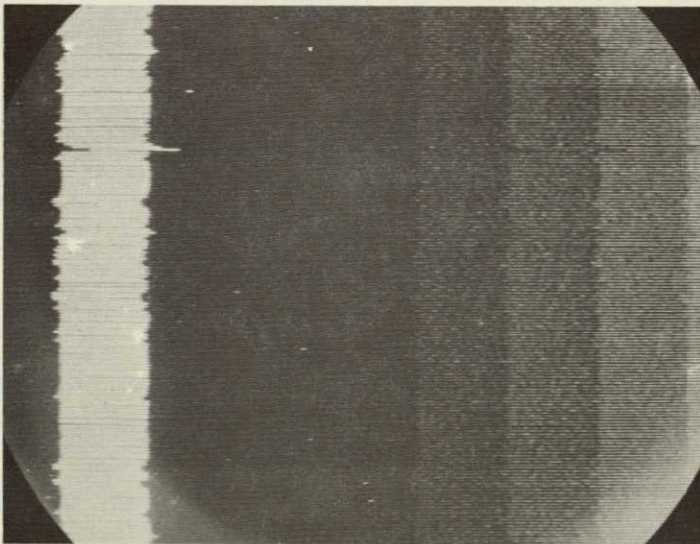
Figure 5-31 CSM Mode 4: TV Picture Quality Tests

$SNR_{IN} = 7 \text{ dB}$ WITH CLICK ELIMINATION



$\Delta f = 1.0 \text{ MHz}$
 $BW_{IF} = 4.9 \text{ MHz}$
 $BW_o = 500 \text{ KHz}$

Figure 5-32 CSM Mode 4: TV Picture Quality Tests
 $SNR_{IN} = 6 \text{ dB}$ WITHOUT CLICK ELIMINATION



$\Delta f = 1.0 \text{ MHz}$
 $BW_{IF} = 4.9 \text{ MHz}$
 $BW_o = 500 \text{ KHz}$

Figure 5-33 CSM Mode 4: TV Picture Quality Tests
 $SNR_{IN} = 6 \text{ dB}$ WITH CLICK ELIMINATION

5.5 TELEVISION PICTURE QUALITY ANALYSIS (Cont'd)

6 dB, the efficiency of the device decreases as a result of circuit saturation. The ability of the device to eliminate noise spikes is primarily related to the click rate and the recovery time of the detection circuitry.

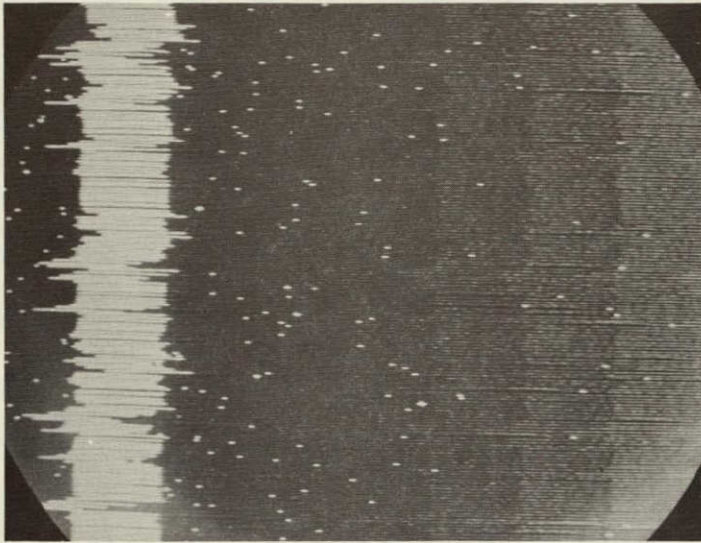
In Figure 5-34 the number of click-produced white spots (before elimination) is considerably greater than the number found in previous pictures, which indicates that the demodulator is beginning to operate below threshold.

Figure 5-35 shows the effect of click elimination on the output signal for a 5-dB input SNR. The click rate is such that approximately 10 percent of the impulse noise perturbations remain after the elimination process. However, the improvement in picture quality due to the click elimination process is still significant.

The effectiveness of the modulation insertion circuitry incorporated in the device can be seen by comparing Figures 5-36 and 5-37. In Figure 5-36 the demodulated signal information is almost completely masked by the perfusion of impulse noise. The line synchronization is also perturbed for most of the frame duration. Figure 5-37 however, displays a demodulated signal that is considerably more intelligible than that of the previous figure. The number of missed line synchronizations is also drastically reduced.

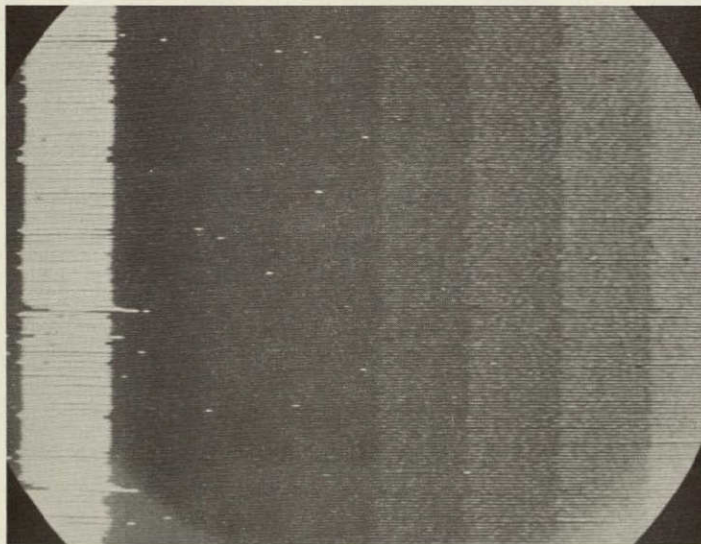
A similar evaluation of the modulation preservation action can be obtained by comparing Figures 5-38 and 5-39 for an input SNR of 3 dB. The grey scale pattern is not visible in Figure 5-38 due to the presence of click noise whereas in Figure 5-39 it is possible to distinguish the individual vertical bars from the remaining noise. The improved line synchronization also contributes to the overall image enhancement obtained with the click eliminator.

Figures 5-40 and 5-41 represent the output of the system for an input SNR of 2 dB. The grey scale modulation is completely masked by the impulse noise as shown in Figure 5-40. The click eliminated output shown in Figure 5-41 contains considerably less noise, but the grey scale vertical bars are still not intelligible. It appears, therefore, that the modulation insertion operation has become ineffective for this low value of input SNR. This observation is correct since previous results have shown that the high click rate which occurs at low input SNR's causes the click eliminator to turn off the output of the demodulator at a rate approaching the modulation frequency.



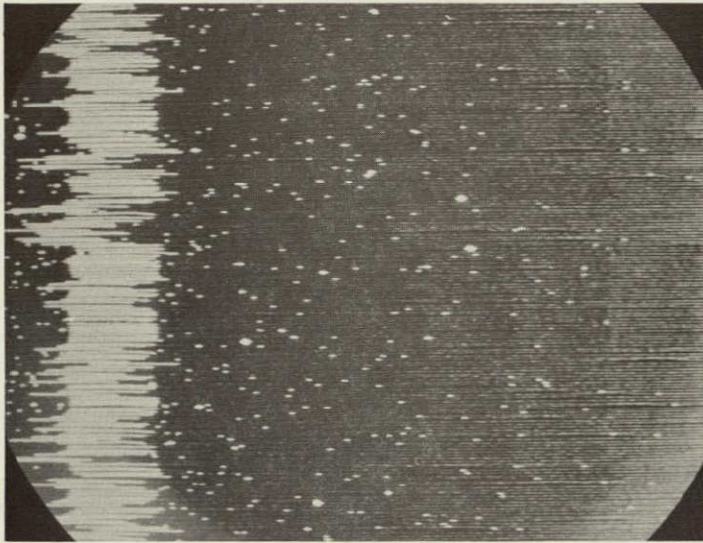
$\Delta f = 1.0 \text{ MHz}$
 $BW_{IF} = 4.9 \text{ MHz}$
 $BW_0 = 500 \text{ KHz}$

Figure 5-34 CSM Mode 4: TV Picture Quality Tests
 $SNR_{IN} = 5 \text{ dB}$ WITHOUT CLICK ELIMINATION



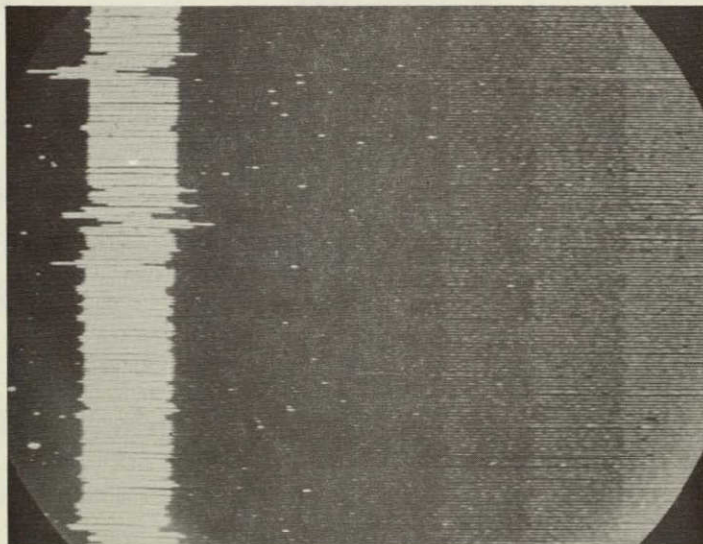
$\Delta f = 1.0 \text{ MHz}$
 $BW_{IF} = 4.9 \text{ MHz}$
 $BW_0 = 500 \text{ KHz}$

Figure 5-35 CSM Mode 4: TV Picture Quality Tests
 $SNR_{IN} = 5 \text{ dB}$ WITH CLICK ELIMINATION



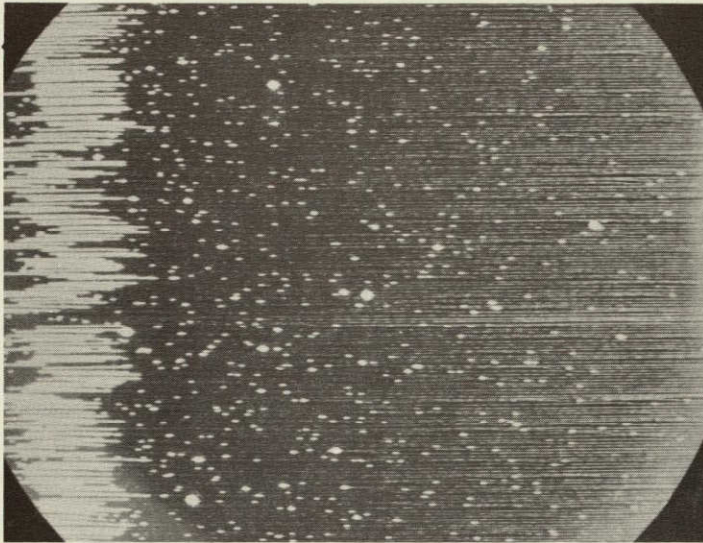
$\Delta f = 1.0 \text{ MHz}$
 $BW_{IF} = 4.3 \text{ MHz}$
 $BW_o = 500 \text{ KHz}$

Figure 5-36 CSM Mode 4: TV Picture Quality Tests
 $SNR_{IN} = 4 \text{ dB}$ WITHOUT CLICK ELIMINATION



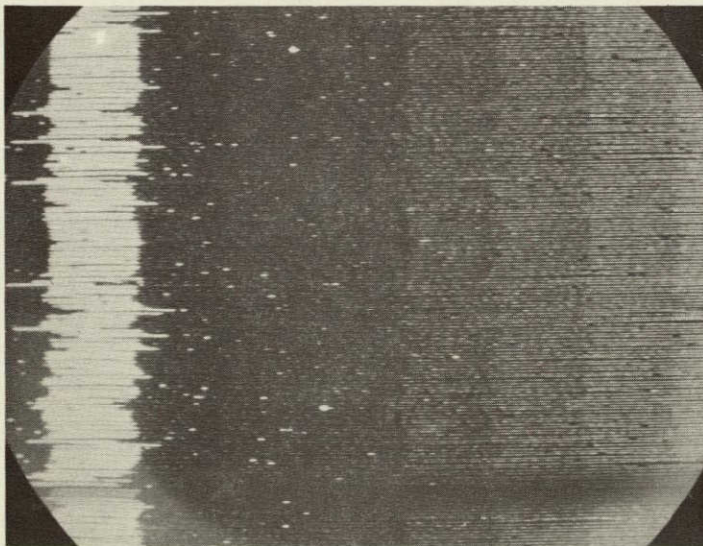
$\Delta f = 1.0 \text{ MHz}$
 $BW_{IF} = 4.3 \text{ MHz}$
 $BW_o = 500 \text{ KHz}$

Figure 5-37 CSM Mode 4: TV Picture Quality Tests
 $SNR_{IN} = 4 \text{ dB}$ WITH CLICK ELIMINATION



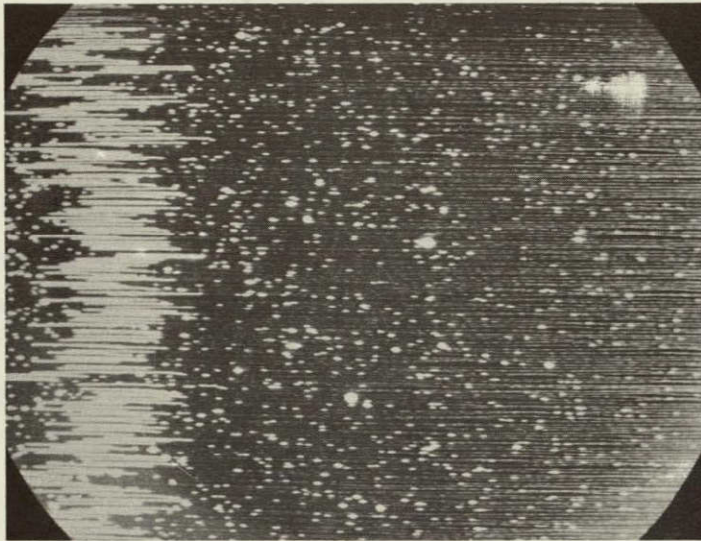
$\Delta f = 1.0 \text{ MHz}$
 $BW_{IF} = 4.9 \text{ MHz}$
 $BW_o = 500 \text{ KHz}$

Figure 5-38 CSM Mode 4: TV Picture Quality Tests
 $SNR_{IN} = 3 \text{ dB}$ WITHOUT CLICK ELIMINATION



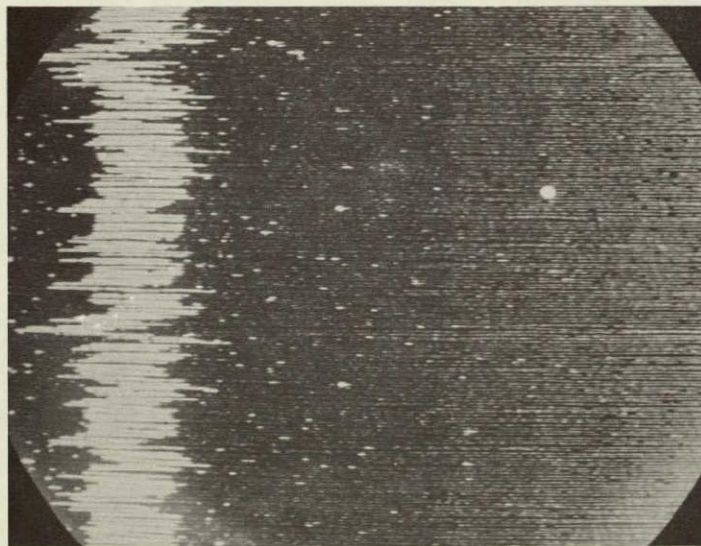
$\Delta f = 1.0 \text{ MHz}$
 $BW_{IF} = 4.9 \text{ MHz}$
 $BW_o = 500 \text{ KHz}$

Figure 5-39 CSM Mode 4: TV Picture Quality Tests
 $SNR_{IN} = 3 \text{ dB}$ WITH CLICK ELIMINATION



$\Delta f = 1.0 \text{ MHz}$
 $BW_{IF} = 4.9 \text{ MHz}$
 $BW_0 = 500 \text{ KHz}$

Figure 5-40 CSM Mode 4: TV Picture Quality Tests
 $SNR_{IN} = 2 \text{ dB}$ WITHOUT CLICK ELIMINATION



$\Delta f = 1.0 \text{ MHz}$
 $BW_{IF} = 4.9 \text{ MHz}$
 $BW_0 = 500 \text{ KHz}$

Figure 5-41 CSM Mode 4: TV Picture Quality Tests
 $SNR_{IN} = 2 \text{ dB}$ WITH CLICK ELIMINATION

5 5 TELEVISION PICTURE QUALITY ANALYSIS (Cont'd)

This implies that the modulation tracking circuitry in the device does not have sufficient time to obtain an accurate estimate of the modulation amplitude between successive click events. This situation is not so much a limitation of the threshold extension device as it is a consequence of having a click rate approach the modulation frequency in the demodulator output.

APPENDIX A

BIBLIOGRAPHY

- Clarke, K , R. Pickholtz, and D Schilling, *A Space Communications Study--Final Report--September 1966-September 1967* Prepared for NASA Electronics Research Center under NASA Grant NGR-33-006.020.
- Clarke, K , K, and D. T Hess, "Frequency Locked Loop FM Demodulator," *IEEE Transactions on Communications Technology*, Vol COM-15, No. 4 August 1967
- Dawson, C. *A Performance Analysis of the Apollo Unified S-Band Communications System for a Typical Lunar Mission.* MSC Internal Note MSC-EB-R-67-1, August 1967.
- Downing, J. *Modulation Systems and Noise* Englewood Cliffs, New Jersey Prentice-Hall, Inc , 1964
- Enloe, L H "Decreasing the Threshold in FM by Frequency Feedback", *Proceedings of IRE*, Vol 50, January 1962.
- Hess, D T , "Cycle Slipping in First Order Phase Locked Loop", *IEEE Transactions on Communications Technology*, April, 1968
- Rice, S O , "Noise in FM Receivers " *Proceedings, Symposium on Time Series Analysis* M Rosenblatt, Editor New York John Wiley & Sons, Inc , 1963.
- Schwartz, M , W Bennet, and S. Stein , *Communications Systems and Techniques* New York McGraw Hill, 1966

APPENDIX B

ABBREVIATIONS AND SYMBOLS

A	Carrier Amplitude
AMP	Amplifier
ATTEN	Attenuator
BW	Bandwidth
BW _{IF}	Predetection (input) Bandwidth
BW _O	Postdetection (output) Bandwidth
cm	Centimeter
CSM	Command/Service Module
dB	Decibel
dBm	Decibel, referenced to 1 milliwatt
DEM0D	Demodulator
DSE	Data Storage Equipment
ESCL	Electronic Systems Compatibility Laboratory
FM	Frequency Modulation
fm	Modulation Frequency in Cycles per Second
FMFB	Frequency Modulation Feedback Discriminator
f _o	Reference or Center Frequency in Cycles per Second
GEN	Generator
G(t)	Unmodulated Carrier
Hz	Hertz
IF	Intermediate Frequency
ISD	Information Systems Division
ISO AMP	Isolation Amplifier
K	Boltzman's Constant (1.38×10^{-23} Watts-sec °K ⁻¹)

KHz	Kilohertz
K_D	Discriminator Constant
LM	Lunar Module
MHz	Megahertz
MSC	Manned Spacecraft Center
MSFN	Manned Space Flight Network
$m(t)$	Modulating Signal
mv	Millivolt
N^+	Positive Click Rate
N^-	Negative Click Rate
N_C	Output Click Noise Power
N_1	Input Noise Power
NM	Nautical Miles
N_O	Output Gaussian Noise Power
N'_O	Total Output Noise Power
$N(t)$	Discriminator input Noise
OSC	Oscillator
PA	Power Amplifier
PLL	Phase Lock Loop
PMP	Pre-Modulation Processor
R	Resultant Carrier Plus Noise Magnitude
r	Radius of Gyration of the Power Spectrum about its Axis of Symmetry
RCVR	Receiver
RF	Radio Frequency
RMS	Root-Mean-Square
sec	Second
S_1	Input Signal Power

SNR	Signal-to-Noise Ratio
SNR _{IN}	Input (Predetection) Signal-to-Noise Ratio
SNR _{OUT}	Output (Postdetection) Signal-to-Noise Ratio
S _o	Output Signal Power
T	System Temperature
TRIPLX	Triplexer
TV	Television
USB	Unified S-Band
XMIT	Transmitter
X(t), Y(t)	Independent Random Variables, Representing the Magnitude of the In-Phase and Quadrature Phase Components of N(t).
β	Modulation Index
Δf	Frequency Deviation
Δφ	Phase Difference between the Resultant Signal plus Noise Vector and the Carrier Vector at t ₁ and t ₂ .
Δω	Radian Frequency Deviation
μsec	Microsecond
τ	Time Interval
φ	Phase of the Resultant Signal-plus-Noise Vector with Respect to the Carrier Vector
φ _e	Phase Error caused by the Noise Disturbance about the Carrier Frequency.
ω _c	Radian Carrier Frequency
ω _e	Radian Frequency Error caused by the Noise Disturbance about the Carrier Frequency.
ω _m	Modulation Frequency in Radians per Second
ω _o	Reference or Center Frequency in Radians per Second